

# Fractional modelling and optimal control strategies for mutated COVID-19 pandemic

Weiyan Ma<sup>1</sup>, Nuri Ma<sup>1</sup>, Changping Dai<sup>1</sup>, YangQuan Chen<sup>2</sup>, and Xinwei Wang<sup>3</sup>

<sup>1</sup>Northwest Minzu University

<sup>2</sup>University of California Merced

<sup>3</sup>Dalian University of Technology

October 24, 2022

## Abstract

As the COVID-19 continues to mutate, the number of infected people is increasing dramatically, and the vaccine is not enough to fight the mutated strain. In this paper, a SEIR-type fractional model with reinfection and vaccine inefficacy is proposed, which can successfully capture the mutated COVID-19 pandemic. The existence, uniqueness, boundedness and nonnegativeness of the fractional model are derived. Based on the basic reproduction number  $R_0$ , locally stability and globally stability are analyzed. The sensitivity analysis evaluate the influence of each parameter on the  $R_0$  and rank key epidemiological parameters. Finally, the necessary conditions for implementing fractional optimal control are obtained by Pontryagin's Maximum Principle, and the corresponding optimal solutions are derived for mitigation COVID-19 transmission. The numerical results show that humans will coexist with COVID-19 for a long time under the current control strategy. Furthermore, it is particularly important to develop new vaccines with higher protection rates.

**SPECIAL ISSUE PAPER**

# Fractional modelling and optimal control strategies for mutated COVID-19 pandemic

Weiyuan Ma\*<sup>1</sup> | Nuri Ma<sup>1</sup> | Changping Dai<sup>1</sup> | YangQuan Chen<sup>2</sup> | Xinwei Wang<sup>3</sup>

<sup>1</sup>School of Mathematics and Computer Science, Northwest Minzu University, Lanzhou 730000, Gansu, China

<sup>2</sup>Mechatronics, Embedded Systems and Automation Lab, University of California, Merced, CA 95343, USA

<sup>3</sup>Department of Engineering Mechanics, State Key Laboratory of Structural Analysis for Industrial Equipment, Dalian University of Technology, Dalian, Liaoning 116024, China

**Correspondence**

\*Weiyuan Ma, School of Mathematics and Computer Science, Northwest Minzu University, Lanzhou 730000, Gansu, China. Email: mwy2004@126.com

**Summary**

As the COVID-19 continues to mutate, the number of infected people is increasing dramatically, and the vaccine is not enough to fight the mutated strain. In this paper, a SEIR-type fractional model with reinfection and vaccine inefficacy is proposed, which can successfully capture the mutated COVID-19 pandemic. The existence, uniqueness, boundedness and nonnegativeness of the fractional model are derived. Based on the basic reproduction number  $R_0$ , locally stability and globally stability are analyzed. The sensitivity analysis evaluate the influence of each parameter on the  $R_0$  and rank key epidemiological parameters. Finally, the necessary conditions for implementing fractional optimal control are obtained by Pontryagin's Maximum Principle, and the corresponding optimal solutions are derived for mitigation COVID-19 transmission. The numerical results show that humans will coexist with COVID-19 for a long time under the current control strategy. Furthermore, it is particularly important to develop new vaccines with higher protection rates.

**KEYWORDS:**

fractional order, COVID-19 model, virus variation, optimal control

## 1 | INTRODUCTION

At the end of 2019, COVID-19, which is caused by severe acute respiratory syndrome coronavirus 2 (SARS-CoV-2), has been identified for the first time.<sup>1</sup> Since then, confirmed cases have been reported in almost all countries and regions around the world. The virus has already caused a serious impact on the global economy and people's health.<sup>2</sup> Governments have adopted all kinds of measures to combat the pandemic, such as social distancing restrictions, wearing masks, vaccinations, etc. More worryingly, the COVID-19 has continued to mutate and acquired numerous mutations, such as Alpha (B.1.1.7), Beta (B.1.351), Delta (B.1.617.2) and Omicron (B.1.1.529). It is worth noting that part of variants have conferred the virus to spread faster and evaded immune responses caused by previous infections or vaccinations.<sup>3</sup> Due to the strong transmissibility ability of some variants, the rate of reinfection has increased significantly, which has been reported between less than 0.5% to more than 5% in different countries.<sup>4</sup>

COVID-19 vaccines act as umbrella to fight the disease because of the immune response produceakes the vaccine insufficient to protect against infection.<sup>5</sup> Some variants are able to evade immunity from vaccines and cause the existing vaccines to be less effective. For example, the study showed that Omicron reduced vaccine effectiveness against infection to 33%.<sup>6</sup> As the virus evolves into many variants and vaccines are becoming less d from a small amount of the virus. It used to be thought that peoples who were vaccinated would be completely protected, but now the mutation meffective, we must take more effective control strategies to prevent the spread of the disease.

Mathematical model is one of the most effective tools to study the pathogenesis, infection law and development trend of COVID-19, which provides great help for governments to formulate comprehensive prevention and control strategies. Peng et al.<sup>7</sup> developed a generalized SEIR model to predict the inflection point in China. Odagaki et al.<sup>8</sup> constructed a SIRQ model which concluded that isolation measures are more effective than lockdown measures. Tang et al.<sup>9</sup> presented an extended SEIR model and assessed the impact of public health interventions on the infection. Ma et al.<sup>10</sup> proposed a SEIR-type model which obtained that contacting distance and immigration rate play an important role in the control of COVID-19. For more works that discuss the modelling and controlling of COVID-19 transmission, please refer to the references.<sup>11,12,13,14</sup>

Fractional models are not only the extension of integer-order models, but also can carry information from population memory and learning mechanisms that can affect COVID-19 spread.<sup>15,16</sup> That is to say, fractional epidemic models can accurately describe the long memory characteristic of the disease. Most recently, Lu et al.<sup>17</sup> proposed a fractional SEIHDR model with the coupling effect of inter-city networks to predict trends in the spread of COVID-19. Baleanu et al.<sup>18</sup> developed a generalized fractional model including isolation and quarantine. Ma et al.<sup>19</sup> investigated a two-sided fractional model and the impact of non-pharmaceutical interventions on the disease transmission. Oud et al.<sup>20</sup> established a fractional model with environmental viral load and found that reducing the rate at which asymptomatic infections release viruses can effectively reduce control costs.

Optimal control is a useful mathematical technique derived from variational method, which is helpful to find some effective strategies for alleviating diseases. Khatun et al.<sup>21</sup> applied the optimal control theory to determine the defense effect of immunoenhancing drugs of leukemia. Xue et al.<sup>22</sup> found that using bed nets, promoting the awareness of humans, and suppressing mosquito populations can effectively suppress of the dengue transmission. Oke et al.<sup>23</sup> developed optimal control strategies to reduce the number of cancer cells by breast cancer models. Zheng et al.<sup>24</sup> gave an optimal strategy to against COVID-19 in refugee camps. Furthermore, fractional optimal control problems have been applied to many different fields, such as diffusion processes, process control, and dynamic control systems<sup>25</sup>. In particular, some diseases have been discussed by using optimal control theory and fractional models, such as HIV/AIDS<sup>26</sup>, TB<sup>27</sup>, and diabetes and tuberculosis co-existence.<sup>28</sup>

As the virus continues to mutate, it is urgent to build new models for reinfection rates rise and vaccine protection rates decline. The main purpose of this paper is to establish a novel fractional model to describe the spread of mutated COVID-19, and therefore to study the appropriate control strategies to minimize the control cost. The main contributions are summarized as follows:

1. A new fractional SEIR-type model with vaccination and virus variation is developed, which can more accurately describe evolution of COVID-19. The modeling idea will help relevant departments and scholars study the spread of the epidemic more clearly.
2. Based on the basic reproduction number  $R_0$ , the local asymptotic stability of disease-free equilibrium and local equilibrium are demonstrated. Furthermore, by constructing proper Lyapunov functions, sufficient conditions for the global asymptotic stability of two equilibriums are established.
3. From the real data of COVID-19, the best-fit values of the parameters are obtained by the fractional Adams-Bashforth-Moulton method and nonlinear least squares. The impact of different vaccine inefficacy and reinfection rates on the spread of COVID-19 are ascertained.
4. Fractional optimal control is used to analyze the proposed model, and the corresponding optimal solution is derived by the Pontryagin's maximum principle. Combined with the current epidemic situation, the cost of non-pharmaceutical interventions and vaccination are considered comprehensively.

This article is organized as follows. In Section 2, some basic definitions and lemmas are given. In Section 3, a model is proposed. In Section 4, dynamic behaviors of the model are analyzed. In Section 5, numerical simulation is given. In Section 6, the existence and solution of the optimal control problem are derived. Section 7 concludes the paper.

## 2 | PRELIMINARY DEFINITIONS AND LEMMAS

In this section, the definition of fractional derivative and some properties are introduced, which will be used in the following part.

**Definition 1** (Li et al<sup>29</sup>). The Caputo fractional derivative  ${}^C D_t^q$  is defined by:

$${}^C D_t^q f(t) = \frac{1}{\Gamma(n-q)} \int_0^t (t-\tau)^{n-q-1} f^{(n)}(\tau) d\tau, \quad (1)$$

where  $n \in \mathbb{N}$  and  $n - 1 < q \leq n$ .

**Lemma 1** (Li et al<sup>29</sup>). Let  $f(t, x)$  be a real-valued continuous function. Consider the system

$${}_0^C D_t^q x(t) = f(t, x), \quad t > t_0, \quad (2)$$

where  $q \in (0, 1)$ , with initial condition  $x(t_0)$ . If  $f(t, x)$  in (2) satisfies the locally Lipschitz condition with respect to  $x$ , then there exists a unique solution of system (2) on  $[t_0, +\infty) \times \Omega$  and  $\Omega \subseteq \mathbb{R}^n$ .

**Lemma 2** (Vargas-De-León<sup>30</sup>). Let  $x(t) \in \mathbb{R}^+$  be a continuous and derivable function. Then

$${}_0^C D_t^q \left( x(t) - x^* - x^* \ln \frac{x(t)}{x^*} \right) \leq \left( 1 - \frac{x^*}{x(t)} \right) {}_0^C D_t^q x(t), \quad (3)$$

where  $t \geq t_0$ ,  $q \in (0, 1)$  and  $x^* \in \mathbb{R}^+$ .

**Lemma 3** (Ameen et al<sup>31</sup>). Let  $t > 0$ ,  $n - 1 < \alpha \leq n$ ,  $n \in \mathbb{N}$ . Then, the following relations hold:

$$\begin{aligned} {}_{t_0} D_t^\alpha f(t) &= {}_{t_0}^C D_t^\alpha f(t) + \sum_{k=0}^{n-1} \frac{f^{(k)}(t_0)}{\Gamma(k - \alpha + 1)} (t - t_0)^{k-\alpha}, \\ {}_T D_T^\alpha f(t) &= {}_T^C D_T^\alpha f(t) + \sum_{k=0}^{n-1} \frac{f^{(k)}(T)}{\Gamma(k - \alpha + 1)} (T - t)^{k-\alpha}, \end{aligned} \quad (4)$$

therefore, if  $f(t_0) = f'(t_0) = f''(t_0) = \dots = f^{(n-1)}(t_0) = 0$ , then  ${}_{t_0} D_t^\alpha f(t) = {}_{t_0}^C D_t^\alpha f(t)$ , if  $f(T) = f'(T) = f''(T) = \dots = f^{(n-1)}(T) = 0$ , then  ${}_T D_T^\alpha f(t) = {}_T^C D_T^\alpha f(t)$ , where  ${}_{t_0} D_t^\alpha$  is the Riemann-Liouville derivative.

### 3 | MATHEMATICAL MODELLING

COVID-19 has had a significant impact on global economic growth and people's healthy. With the mutation of the virus, some new features have emerged in the development of the COVID-19. Vaccine can not provide 100% protection against the disease, that is people who are vaccinated can still get infected. Besides that, peoples who recovered from COVID-19 can be reinfected. In order to face this situation, it is important to establish appropriate models.

In this work, the total population  $N(t)$  is divided into seven classes, that is susceptible  $S(t)$ , vaccination  $V(t)$ , exposure  $E(t)$ , infection  $I(t)$ , quarantine  $Q(t)$ , recovery  $R(t)$  and death  $D(t)$ . Figure 1 shows a flow chart of the disease. The susceptible individuals are vaccinated with the rate  $\delta$ . The vaccinated individuals are infected with the rate  $\alpha_2$ . The transfer rate from susceptible to infected individuals is  $\alpha_1$ . Exposed individuals complete their incubation period and enter infected class at a rate of  $\gamma$ . The infected individuals are quarantined at the rate of  $\beta$ . The recovery and mortality rates for these quarantine individuals are  $\lambda$  and  $\kappa$ , respectively. The natural mortality rate is represented by the symbol  $\mu$ , and the recruitment rate or birth rate is represented by the symbol  $\Lambda$ . The  $\alpha_3$  is the reinfected rate from recovered individuals to exposed class. Here, if  $\alpha_3 = 0$  means that the recovered individual not be reinfected, while  $\alpha_3 = 1$  implies that the recovered individual have a 100% risk of reinfection. The biological significance of the parameters is given in Table 1. Therefore, fractional model can be written as follows:

$$\begin{aligned} {}_0^C D_t^q S(t) &= \Lambda - \alpha_1 S(t)I(t) - \delta S(t) - \mu S(t), \\ {}_0^C D_t^q V(t) &= \delta S(t) - \alpha_2 V(t)I(t) - \mu V(t), \\ {}_0^C D_t^q E(t) &= \alpha_1 S(t)I(t) + \alpha_2 V(t)I(t) + \alpha_3 R(t)I(t) - \gamma E(t) - \mu E(t), \\ {}_0^C D_t^q I(t) &= \gamma E(t) - \beta I(t) - \mu I(t), \\ {}_0^C D_t^q Q(t) &= \beta I(t) - \lambda Q(t) - \kappa Q(t) - \mu Q(t), \\ {}_0^C D_t^q R(t) &= \lambda Q(t) - \alpha_3 R(t)I(t) - \mu R(t), \\ {}_0^C D_t^q D(t) &= \kappa Q(t). \end{aligned} \quad (5)$$

The initial conditions are given as follows:

$$S(t_0) \geq 0, \quad E(t_0) \geq 0, \quad I(t_0) \geq 0, \quad Q(t_0) \geq 0, \quad R(t_0) \geq 0, \quad V(t_0) \geq 0, \quad D(t_0) \geq 0. \quad (6)$$

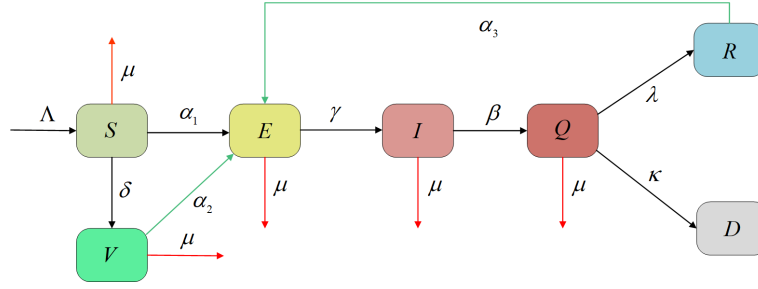


**Figure 1** Schematic diagram of the fractional model (5)

**Table 1** Model parameters and their biological significance.

Parameters	Epidemiological description	Dimension/Unit
$\Lambda$	Recruitment rate	Population/Day <sup>-1</sup>
$\delta$	Vaccination rate	Day <sup>-1</sup>
$\alpha_1$	Infection rate	Day <sup>-1</sup>
$\alpha_2$	Vaccine inefficacy	Day <sup>-1</sup>
$\alpha_3$	Reinfection rate	Day <sup>-1</sup>
$\gamma$	Latent time	Day <sup>-1</sup>
$\beta$	Quarantine time	Day <sup>-1</sup>
$\lambda$	Cure rate	Day <sup>-1</sup>
$\kappa$	Disease-related mortality	Day <sup>-1</sup>
$\mu$	Natural mortality rate	Population/Day <sup>-1</sup>

## 4 | MODEL ANALYSIS

In this section, existence, uniqueness, boundedness and non-negativity of the solutions for fractional SEIR-type model (5) are investigated. Besides that, stability analysis of model (5) is also derived.

### 4.1 | Existence and uniqueness

**Theorem 1.** For each nonnegative initial conditions  $(S_0, V_0, E_0, I_0, Q_0, R_0, D_0) \in \mathbb{R}^7$ , then there exists a unique solution of fractional model (5).

**proof.** Let  $\Omega = \{(S, V, E, I, Q, R, D) \in \mathbb{R}^7 : \max\{|S|, |V|, |E|, |I|, |Q|, |R|, |D|\} \leq \rho\}$ . Define a mapping  $M(X) = (M_1(X), M_2(X), M_3(X), M_4(X), M_5(X), M_6(X), M_7(X))$ , and

$$\begin{aligned}
 M_1(X) &= \Lambda - \alpha_1 SI - \delta S - \mu S, \\
 M_2(X) &= \delta S - \alpha_2 VI - \mu V, \\
 M_3(X) &= \alpha_1 SI + \alpha_2 VI + \alpha_3 RI - \gamma E - \mu E, \\
 M_4(X) &= \gamma E - \beta I - \mu I, \\
 M_5(X) &= \beta I - \lambda Q - \kappa Q - \mu Q, \\
 M_6(X) &= \lambda Q - \alpha_3 RI - \mu R, \\
 M_7(X) &= \kappa Q,
 \end{aligned}$$

where  $X = (S, V, E, I, Q, R, D) \in \Omega$ .

For any  $X, \bar{X} \in \Omega$ , we have

$$\begin{aligned}
& \| M(X) - M(\bar{X}) \| \\
& = |M_1(X) - M_1(\bar{X})| + |M_2(X) - M_2(\bar{X})| + |M_7(X) - M_7(\bar{X})| \\
& \leq |\Lambda - \alpha_1 S I - \delta S - \mu S - \Lambda + \alpha_1 \bar{S} \bar{I} + \delta \bar{S} + \mu \bar{S}| + |\delta S - \alpha_2 V I - \mu V - \delta \bar{S} + \alpha_2 \bar{V} \bar{I} + \mu \bar{V}| \\
& \quad + |\alpha_1 S I + \alpha_2 V I + \alpha_3 R I - \gamma E - \mu E - \alpha_1 \bar{S} \bar{I} - \alpha_2 \bar{V} \bar{I} - \alpha_3 \bar{R} \bar{I} + \gamma \bar{E} + \mu \bar{E}| \\
& \quad + |\gamma E - \beta I - \mu I - \gamma \bar{E} + \beta \bar{I} + \mu \bar{I}| + |\beta I - \lambda Q - \kappa Q - \mu Q - \beta \bar{I} + \lambda \bar{Q} + \kappa \bar{Q} + \mu \bar{Q}| \\
& \quad + |\lambda Q - \alpha_3 R I - \mu R - \lambda \bar{Q} + \alpha_3 \bar{R} \bar{I} + \mu \bar{R}| + |\kappa Q - \kappa \bar{Q}| \\
& \leq (2\alpha_1 \rho + 2\delta + \mu) |S - \bar{S}| + (2\alpha_2 \rho + \mu) |V - \bar{V}| + (2\gamma + \mu) |E - \bar{E}| \\
& \quad + (2\rho(\alpha_1 + \alpha_2 + \alpha_3) + 2\beta + \mu) |I - \bar{I}| + (2\lambda + 2\kappa + \mu) |Q - \bar{Q}| + (2\alpha_3 \rho + \mu) |R - \bar{R}| \\
& \leq L \| X - \bar{X} \|,
\end{aligned}$$

where

$$L = \max\{2\alpha_1 \rho + 2\delta + \mu, 2\alpha_2 \rho + \mu, 2\gamma + \mu, 2\beta + \mu + 2\rho(\alpha_1 + \alpha_2 + \alpha_3), 2\lambda + 2\kappa + \mu, 2\alpha_3 \rho + \mu\}.$$

That is  $M(X)$  satisfies the Lipschitz condition. According to Lemma 1, model (5) has a unique solution.

## 4.2 | Boundedness and nonnegativity

The last equation of recovered individuals  $D(t)$  in system (5) is independent of other equations. System (5) can be reduced to the following form:

$$\begin{aligned}
{}_0^C D_t^q S(t) &= \Lambda - \alpha_1 S(t)I(t) - \delta S(t) - \mu S(t), \\
{}_0^C D_t^q V(t) &= \delta S(t) - \alpha_2 V(t)I(t) - \mu V(t), \\
{}_0^C D_t^q E(t) &= \alpha_1 S(t)I(t) + \alpha_2 V(t)I(t) + \alpha_3 R(t)I(t) - \gamma E(t) - \mu E(t), \\
{}_0^C D_t^q I(t) &= \gamma E(t) - \beta I(t) - \mu I(t), \\
{}_0^C D_t^q Q(t) &= \beta I(t) - \lambda Q(t) - \kappa Q(t) - \mu Q(t), \\
{}_0^C D_t^q R(t) &= \lambda Q(t) - \alpha_3 R(t)I(t) - \mu R(t).
\end{aligned} \tag{7}$$

**Theorem 2.** The solutions of fractional model (7) are uniformly bounded and nonnegative for  $t > 0$ .

**proof.** Let  $N(t) = S(t) + V(t) + E(t) + I(t) + Q(t) + R(t)$ . From equation (7), one has

$${}_0^C D_t^q N(t) \leq \Lambda - \mu N(t). \tag{8}$$

Using the comparison principle<sup>32</sup> of fractional system, one derives

$$\begin{aligned}
N(t) &\leq \Lambda t^q E_{q,q+1}(-\mu t^q) + N(0) E_{q,1}(-\mu t^q) \\
&= \frac{\Lambda}{\mu} - \frac{\Lambda}{\mu} E_{q,1}(-\mu t^q) + N(0) E_{q,1}(-\mu t^q).
\end{aligned}$$

where  $E_{q,1}$  is the Mittag-Leffler function. From  $\lim_{t \rightarrow \infty} E_{q,1}(-\mu t^q) = 0$ , one gets

$$N(t) \leq \frac{\Lambda}{\mu}, \text{ as } t \rightarrow \infty.$$

Thus, all the solutions of fractional model (7) are confined to the region

$$\Theta = \{(S, V, E, I, Q, R) \in \mathbb{R}_+^6 : N(t) \leq \frac{\Lambda}{\mu} + \varepsilon, \varepsilon > 0\}.$$

In the subsequent, we will prove that the solutions of fractional model (7) are non-negative.

From the first equation of model (5), we have

$$\begin{aligned}
{}_0^C D_t^q S(t) &= \Lambda - \alpha_1 S I - \delta S - \mu S \\
&\geq -(\alpha_1 I + \delta + \mu) S \\
&\geq -(\alpha_1 \frac{\Lambda}{\mu} + \delta + \mu) S.
\end{aligned}$$

According to the fractional comparison theorem<sup>32</sup>, and the properties of the Mittag-Leffler function<sup>?</sup>, for any  $q \in (0, 1)$ , one gets

$$S(t) \geq S(0)E_{q,1} \left( -(\alpha_1 \frac{\Lambda}{\mu} + \delta + \mu)t^q \right) \Rightarrow S(t) \geq 0.$$

Similarly, one can prove that

$$V(t) \geq V(0)E_{q,1} \left( -(\alpha_2 \frac{\Lambda}{\mu} + \mu)t^q \right) \Rightarrow V(t) \geq 0,$$

$$E(t) \geq E(0)E_{q,1} (-(\gamma + \mu)t^q) \Rightarrow E(t) \geq 0,$$

$$I(t) \geq I(0)E_{q,1} (-(\beta + \mu)t^q) \Rightarrow I(t) \geq 0,$$

$$Q(t) \geq Q(0)E_{q,1} (-(\lambda + \kappa + \mu)t^q) \Rightarrow Q(t) \geq 0,$$

$$R(t) \geq R(0)E_{q,1} \left( -(\alpha_3 \frac{\Lambda}{\mu} + \mu)t^q \right) \Rightarrow R(t) \geq 0.$$

Thus, the solution of fractional model (7) is nonnegative. All this completes the proof.

### 4.3 | The basic reproduction number $R_0$

Let  $P_F = (S^*, V^*, E^*, I^*, Q^*, R^*)$  be the disease-free equilibrium of (7). Then, we have

$$P_F = \left( \frac{\Lambda}{\delta + \mu}, \frac{\delta\Lambda}{\mu(\delta + \mu)}, 0, 0, 0, 0 \right). \quad (9)$$

The next-generation matrix method<sup>33</sup> is used to get  $R_0$ . Obviously,  $E(t)$ ,  $I(t)$  and  $Q(t)$  are the infected compartments. In virtue of (7), we have

$$\begin{aligned} {}_0^C D_t^q E(t) &= \alpha_1 S I + \alpha_2 V I + \alpha_3 R I - \gamma E - \mu E, \\ {}_0^C D_t^q I(t) &= \gamma E - \beta I - \mu I, \\ {}_0^C D_t^q Q(t) &= \beta I - \lambda Q - \kappa Q - \mu Q. \end{aligned} \quad (10)$$

Then, we derive

$$\mathcal{F}(P_F) = \begin{pmatrix} -\gamma - \mu & \alpha_1 S^* + \alpha_2 V^* & 0 \\ \gamma & -\beta - \mu & 0 \\ 0 & \beta & -\lambda - \kappa - \mu \end{pmatrix}.$$

The matrix  $\mathcal{F}(P_F)$  can be decomposed into  $\mathcal{F}$  and  $\mathcal{V}$ , that is  $\mathcal{F}(P_F) = \mathcal{F} - \mathcal{V}$ , where

$$\mathcal{F} = \begin{pmatrix} 0 & \alpha_1 S^* + \alpha_2 V^* & 0 \\ 0 & 0 & 0 \\ 0 & 0 & 0 \end{pmatrix}, \quad \mathcal{V} = \begin{pmatrix} \gamma + \mu & 0 & 0 \\ -\gamma & \beta + \mu & 0 \\ 0 & -\beta & \lambda + \kappa + \mu \end{pmatrix}.$$

The basic reproduction number  $R_0$  is given by

$$R_0 = \rho(\mathcal{F} \mathcal{V}^{-1}) = \frac{\gamma\Lambda(\alpha_1\mu + \alpha_2\delta)}{\mu(\delta + \mu)(\gamma + \mu)(\beta + \mu)}, \quad (11)$$

where  $\rho(\cdot)$  is the spectral radius.

Surmise that  $P_E = (S^*, V^*, E^*, I^*, Q^*, R^*)$  represents the endemic equilibrium for (7), so that

$$P_E = \left( \frac{\Lambda}{\alpha_1 I^* + A}, \frac{\delta S^*}{\alpha_2 I^* + \mu}, \frac{C I^*}{\gamma}, I^*, \frac{\beta I^*}{D}, \frac{\lambda Q^*}{\alpha_3 I^* + \mu} \right), \quad (12)$$

where  $A = \delta + \mu$ ,  $B = \gamma + \mu$ ,  $C = \beta + \mu$ ,  $D = \lambda + \kappa + \mu$ , and  $I^*$  is a positive roots of the following equation:

$$\frac{\alpha_1 \Lambda}{\alpha_1 I^* + A} + \frac{\alpha_2 \delta \Lambda}{(\alpha_1 I^* + A)(\alpha_2 I^* + \mu)} + \frac{\alpha_3 \lambda \beta I^*}{D(\alpha_3 I^* + \mu)} - \frac{BC}{\gamma} = 0. \quad (13)$$

Equation (13) can be read as

$$f(I^*) = aI^{*3} + bI^{*2} + cI^* + d = 0, \quad (14)$$

where

$$\begin{aligned} a &= \alpha_1 \alpha_2 \alpha_3 \left( \lambda \beta - \frac{BCD}{\gamma} \right), \quad b = \alpha_1 \alpha_2 D \left( \Lambda \alpha_3 - \frac{\mu BC}{\gamma} \right) + \alpha_3 (\alpha_1 \mu + \alpha_2 A) \left( \lambda \beta - \frac{BCD}{\gamma} \right), \\ c &= \alpha_1 \mu \Lambda D (\alpha_2 + \alpha_3) + \alpha_3 \Lambda (\alpha_2 \delta D + \beta \mu A) - \frac{BCD}{\gamma} (\alpha_3 \mu \Lambda + \mu (\alpha_1 \mu + \alpha_2 A)), \\ d &= \frac{\mu^2 ABCD}{\gamma} (R_0 - 1). \end{aligned}$$

The cubic polynomial  $f(I^*)$  has one positive root when the following conditions are hold: (i)  $ad < 0$ ; (ii)  $f'(I^*) < 0$  or  $f'(I^*) > 0$ , and  $f(I_1)f(I_2) > 0$ . Here,  $I_1$  and  $I_2$  are roots of  $f'(I^*) = 0$ . Thus,  $f(I^*)$  has a unique positive root.

#### 4.4 | Local stability

**Theorem 3.** If  $R_0 < 1$ , the disease-free equilibrium  $P_F$  of system (7) is locally asymptotically stable.

**proof.** The Jacobian matrix of system (7) at  $P_F$  arrives to

$$\mathcal{J}(P_F) = \begin{pmatrix} -\delta - \mu & 0 & 0 & \alpha_1 S^* & 0 & 0 \\ \delta & -\mu & 0 & \alpha_2 V^* & 0 & 0 \\ 0 & 0 & -\gamma - \mu & \alpha_1 S^* + \alpha_2 V^* & 0 & 0 \\ 0 & 0 & \gamma & -\beta - \mu & 0 & 0 \\ 0 & 0 & 0 & \beta & -\lambda - \kappa - \mu & 0 \\ 0 & 0 & 0 & 0 & \lambda & -\mu \end{pmatrix}. \quad (15)$$

The eigenvalues of (15) can be obtained from the following equation:

$$(v + \mu)^2 (v + \lambda + \kappa + \mu) (v + \delta + \mu) [v^2 + (2\mu + \beta + \gamma)v + (\beta + \mu)(\gamma + \mu)(1 - R_0)] = 0. \quad (16)$$

The roots of equation (16) are calculated as  $v_1 = v_2 = -\mu$ ,  $v_3 = -\delta - \mu$ ,  $v_4 = -\lambda - \kappa - \mu$ . The remaining two eigenvalues are

$$\begin{aligned} v_5 &= -\frac{1}{2} \left( \sqrt{(2\mu + \beta + \gamma)^2 - 4(\beta + \mu)(\gamma + \mu)(1 - R_0)} + 2\mu + \beta + \gamma \right), \\ v_6 &= -\frac{1}{2} \left( -\sqrt{(2\mu + \beta + \gamma)^2 - 4(\beta + \mu)(\gamma + \mu)(1 - R_0)} + 2\mu + \beta + \gamma \right). \end{aligned}$$

When  $R_0 < 1$ , it is obvious that  $v_5 < 0$  and  $v_6 < 0$ . From<sup>19</sup> and all the eigenvalues satisfy the condition  $|\arg(v_i)| > \frac{\pi}{2}$ ,  $i = 1, 2, \dots, 6$ , the disease-free equilibrium  $P_F$  is locally asymptotically stable.

**Theorem 4.** If  $R_0 > 1$ , then the endemic equilibrium  $P_E$  of system (7) is locally asymptotically stable.

**proof.** Let

$$\begin{aligned} a_{11} &= -(\alpha_1 I^* + \delta + \mu), \quad a_{14} = -\alpha_1 S^*, \quad a_{21} = \delta, \quad a_{22} = -(\alpha_2 I^* + \mu), \quad a_{24} = -\alpha_2 V^*, \quad a_{31} = \alpha_1 I^*, \quad a_{32} = \alpha_2 I^*, \\ a_{33} &= -(\gamma + \mu), \quad a_{34} = \alpha_1 S^* + \alpha_2 V^* + \alpha_3 R^*, \quad a_{36} = \alpha_3 I^*, \quad a_{43} = \gamma, \quad a_{44} = -(\beta + \mu), \quad a_{54} = \beta, \\ a_{55} &= -(\lambda + \kappa + \mu), \quad a_{64} = -\alpha_3 R^*, \quad a_{65} = \lambda, \quad a_{66} = -(\alpha_3 I^* + \mu). \end{aligned}$$

The Jacobian matrix of model (7) at  $P_E$  is given by

$$\mathcal{J}(P_E) = \begin{pmatrix} a_{11} & 0 & 0 & a_{14} & 0 & 0 \\ a_{21} & a_{22} & 0 & a_{24} & 0 & 0 \\ a_{31} & a_{32} & a_{33} & a_{34} & 0 & a_{36} \\ 0 & 0 & a_{43} & a_{44} & 0 & 0 \\ 0 & 0 & 0 & a_{54} & a_{55} & 0 \\ 0 & 0 & 0 & a_{64} & a_{65} & a_{66} \end{pmatrix}.$$

The characteristic equation of  $\mathcal{J}(P_E)$  is

$$v^6 + U_1 v^5 + U_2 v^4 + U_3 v^3 + U_4 v^2 + U_5 v + U_6 = 0,$$

where

$$\begin{aligned}
U_1 &= -(a_{11} + a_{22} + a_{33} + a_{44} + a_{55} + a_{66}), \\
U_2 &= a_{11}(a_{22} + a_{33} + a_{44} + a_{55} + a_{66}) + a_{22}(a_{33} + a_{44} + a_{55} + a_{66}) + a_{33}(a_{44} + a_{55} + a_{66}) + a_{44}a_{55} \\
&\quad + a_{44}a_{66} + a_{55}a_{66} - a_{34}a_{43}, \\
U_3 &= a_{11}(a_{34}a_{43} - a_{22}a_{33} - a_{22}a_{44} - a_{22}a_{55} - a_{22}a_{66} - a_{33}a_{44} - a_{33}a_{55} - a_{33}a_{66} - a_{44}a_{55} - a_{44}a_{66} - a_{55}a_{66}) \\
&\quad + a_{22}(a_{34}a_{43} - a_{33}a_{44} - a_{33}a_{55} - a_{33}a_{66} - a_{44}a_{55} - a_{44}a_{66} - a_{55}a_{66}) + a_{55}(a_{34}a_{43} - a_{33}a_{44} - a_{33}a_{66} \\
&\quad - a_{44}a_{66}) - a_{14}a_{31}a_{43} - a_{24}a_{32}a_{43} - a_{33}a_{44}a_{66} + a_{34}a_{43}a_{66} - a_{36}a_{43}a_{64}, \\
U_4 &= a_{11}(a_{22}a_{33}a_{44} - a_{22}a_{34}a_{43} + a_{24}a_{32}a_{43} + a_{22}a_{33}a_{55} + a_{22}a_{33}a_{66} + a_{22}a_{44}a_{55} + a_{22}a_{44}a_{66} + a_{22}a_{55}a_{66} \\
&\quad + a_{33}a_{44}a_{55} + a_{33}a_{44}a_{66} + a_{33}a_{55}a_{66} - a_{34}a_{43}a_{55} - a_{34}a_{43}a_{66} + a_{36}a_{43}a_{64} + a_{44}a_{55}a_{66}) + a_{22}(a_{14}a_{31}a_{43} \\
&\quad + a_{33}a_{44}a_{55} + a_{33}a_{44}a_{66} + a_{33}a_{55}a_{66} - a_{34}a_{43}a_{55} - a_{34}a_{43}a_{66} + a_{36}a_{43}a_{64} + a_{44}a_{55}a_{66}) + a_{55}(a_{14}a_{31}a_{43} \\
&\quad + a_{24}a_{32}a_{43} + a_{33}a_{44}a_{66} - a_{34}a_{43}a_{66} + a_{36}a_{43}a_{64}) - a_{14}a_{21}a_{32}a_{43} + a_{14}a_{31}a_{43}a_{66} + a_{24}a_{32}a_{43}a_{66} \\
&\quad - a_{36}a_{43}a_{54}a_{65}, \\
U_5 &= a_{11}(a_{22}a_{34}a_{43}a_{55} - a_{22}a_{33}a_{44}a_{55} - a_{22}a_{33}a_{44}a_{66} + a_{22}a_{34}a_{43}a_{66} - a_{22}a_{34}a_{43}a_{55} - a_{22}a_{36}a_{43}a_{64} \\
&\quad - a_{24}a_{32}a_{43}a_{66} - a_{22}a_{33}a_{55}a_{66} - a_{22}a_{44}a_{55}a_{66} - a_{33}a_{44}a_{55}a_{66} + a_{34}a_{43}a_{55}a_{66} + a_{36}a_{43}a_{54}a_{65}) \\
&\quad + a_{14}(a_{21}a_{32}a_{43}a_{55} - a_{22}a_{31}a_{43}a_{55} + a_{21}a_{32}a_{43}a_{66} - a_{22}a_{31}a_{43}a_{66} - a_{31}a_{43}a_{55}a_{66}) \\
&\quad + a_{22}(a_{34}a_{43}a_{55}a_{66} - a_{33}a_{44}a_{55}a_{66} + a_{36}a_{43}a_{54}a_{65} - a_{36}a_{43}a_{55}a_{64}) - a_{24}a_{32}a_{43}a_{55}a_{66}, \\
U_6 &= a_{11}(a_{22}a_{33}a_{44}a_{55}a_{66} - a_{22}a_{34}a_{43}a_{55}a_{66} - a_{22}a_{36}a_{43}a_{54}a_{65} + a_{24}a_{32}a_{43}a_{55}a_{66} + a_{22}a_{36}a_{43}a_{55}a_{64}) \\
&\quad + a_{55}a_{66}(a_{14}a_{22}a_{31}a_{43} - a_{14}a_{21}a_{32}a_{43}).
\end{aligned}$$

For convenience, let

$$\begin{aligned}
\Delta_1 &= |U_1|, \quad \Delta_2 = \begin{vmatrix} U_1 & 1 \\ U_3 & U_2 \end{vmatrix}, \quad \Delta_3 = \begin{vmatrix} U_1 & 1 & 0 \\ U_3 & U_2 & U_1 \\ U_5 & U_4 & U_3 \end{vmatrix}, \\
\Delta_4 &= \begin{vmatrix} U_1 & 1 & 0 & 0 \\ U_3 & U_2 & U_1 & 1 \\ U_5 & U_4 & U_3 & U_2 \\ 0 & U_6 & U_5 & U_4 \end{vmatrix}, \quad \Delta_5 = \begin{vmatrix} U_1 & 1 & 0 & 0 & 0 \\ U_3 & U_2 & U_1 & 1 & 0 \\ U_5 & U_4 & U_3 & U_2 & U_1 \\ 0 & U_6 & U_5 & U_4 & U_3 \\ 0 & 0 & 0 & U_6 & U_5 \end{vmatrix}, \quad \Delta_6 = |J(P_E)|.
\end{aligned}$$

By Routh-Hurwitz criterion, if the following conditions are hold:

$$U_j > 0, \Delta_j > 0, j = 1, 2, \dots, 6,$$

then  $P_E$  is locally asymptotically stable. The proof is completed.

## 4.5 | Global stability

In this part, the global stability of  $P_E$  and  $P_F$  of system (7) is investigated.

**Theorem 5.** If  $R_0 < 1$ , then the disease-free equilibrium  $P_F$  of system (7) is globally asymptotically stable.

**proof.** Construct a Lyapunov function  $L_1(t)$  as follows

$$L_1(t) = S(t) - S_0 - S_0 \ln \frac{S(t)}{S_0} + V(t) - V_0 - V_0 \ln \frac{V(t)}{V_0} + E(t) + \frac{\gamma + \mu}{\gamma} I(t) + \frac{\lambda}{\lambda + \kappa + \mu} Q(t) + R(t).$$

Calculating the  $q$ -order derivative of  $L_1(t)$  along the solution trajectories of (7), from Lemma 2, we get

$$\begin{aligned} {}_0^C D_t^q L_1(t) &\leq \left(1 - \frac{S^*}{S}\right) {}_0^C D_t^q S(t) + \left(1 - \frac{V^*}{V}\right) {}_0^C D_t^q V(t) + {}_0^C D_t^q E(t) + \frac{\gamma + \mu}{\gamma} {}_0^C D_t^q I(t) + {}_0^C D_t^q R(t) + \frac{\lambda}{\lambda + \kappa + \mu} {}_0^C D_t^q Q(t) \\ &= \left(1 - \frac{S^*}{S}\right) (\Lambda - \alpha_1 S I - \delta S - \mu S) + \left(1 - \frac{V^*}{V}\right) (\delta S - \alpha_2 V I - \mu V) + \alpha_1 S I + \alpha_2 V I + \alpha_3 R I \\ &\quad - \gamma E - \mu E + \frac{\gamma + \mu}{\gamma} (\gamma E - \beta I - \mu I) + \frac{\lambda}{\lambda + \kappa + \mu} (\beta I - \lambda Q - \kappa Q - \mu Q) + \lambda Q - \alpha_3 R I - \mu R. \end{aligned}$$

As  $\Lambda = (\delta + \mu)S^*$ , from (11), we obtain

$$\begin{aligned} {}_0^C D_t^q L_1(t) &\leq \left(1 - \frac{S^*}{S}\right) ((\delta + \mu)S^* - \alpha_1 S I - \delta S - \mu S) + \left(1 - \frac{V^*}{V}\right) (\delta S - \alpha_2 V I - \mu V) + \alpha_1 S I + \alpha_2 V I \\ &\quad + \alpha_3 R I - \gamma E - \mu E + \frac{\gamma + \mu}{\gamma} (\gamma E - \beta I - \mu I) + \frac{\lambda}{\lambda + \kappa + \mu} (\beta I - \lambda Q - \kappa Q - \mu Q) + \lambda Q \\ &\quad - \alpha_3 R I - \mu R \\ &\leq \left(1 - \frac{S^*}{S}\right) ((\delta + \mu)S^* - \alpha_1 S I - \delta S - \mu S) + \left(1 - \frac{V^*}{V}\right) (\delta S - \alpha_2 V I - \mu V) + \alpha_1 S I \\ &\quad + \alpha_2 V I - \frac{\gamma + \mu}{\gamma} (\beta I + \mu I) \\ &= -\frac{\delta + \mu}{S} (S - S^*)^2 + \mu V^* \left(2 - \frac{V^*}{V} - \frac{V}{V^*}\right) + \frac{(\beta + \mu)(\gamma + \mu)}{\gamma} (R_0 - 1) I. \end{aligned}$$

Hence,  $R_0 < 1$  implies that

$${}_0^C D_t^q L_1(t) \leq 0, \text{ for all } t \geq 0.$$

Besides that,  ${}_0^C D_t^q L_1(t) = 0$  if and only if  $S(t) = S^*$ ,  $V(t) = V^*$ ,  $E(t) = 0$ ,  $I(t) = 0$ ,  $Q(t) = 0$  and  $R(t) = 0$ . Thus, the largest invariant set in  $\Omega_1 = \{(S^*, V^*, 0, 0, 0, 0) \in \mathbb{R}_+^6 : {}_0^C D_t^q L_1(t) = 0\}$  is  $P_F$ . By the Lemma 4.6 of <sup>34</sup>, we obtain all solutions in  $\Omega_1$  converge to  $P_F$ . Therefore, the  $P_F$  of model (7) is global asymptotically stable. This completes the proof.

**Theorem 6.** If  $R_0 > 1$ , then the endemic equilibrium  $P_E$  of system (7) is globally asymptotically stable.

**proof.** The following relations from system (7) at  $P_E$  can be obtained:

$$\begin{cases} \Lambda = \alpha_1 S^* I^* + \delta S^* + \mu S^*, \\ \delta S^* = \alpha_2 V^* I^* + \mu V^*, \\ (\gamma + \mu)E^* = \alpha_1 S^* I^* + \alpha_2 V^* I^* + \alpha_3 R^* I^*, \\ \gamma E^* = (\beta + \mu)I^*, \\ \beta I^* = (\lambda + \kappa + \mu)Q^*, \\ \lambda Q^* = \alpha_3 R^* I^* + \mu R^*. \end{cases} \quad (17)$$

Then, let us construct a Lyapunov function  $L_2(t)$  as

$$\begin{aligned} L_2(t) &= x_1 \left( S(t) - S^* - S^* \ln \frac{S(t)}{S^*} \right) + x_2 \left( V(t) - V^* - V^* \ln \frac{V(t)}{V^*} \right) + x_3 \left( E(t) - E^* - E^* \ln \frac{E(t)}{E^*} \right) \\ &\quad + x_4 \left( I(t) - I^* - I^* \ln \frac{I(t)}{I^*} \right) + x_5 \left( Q(t) - Q^* - Q^* \ln \frac{Q(t)}{Q^*} \right) + x_6 \left( R(t) - R^* - R^* \ln \frac{R(t)}{R^*} \right). \end{aligned}$$

Calculating the  $q$ -order derivative of  $L_2(t)$  along with the solution trajectories of system (7), it follows from Lemma 2 that

$$\begin{aligned}
{}_0^C D_t^q L_2(t) &\leq x_1 \left(1 - \frac{S^*}{S(t)}\right) {}_0^C D_t^q S(t) + x_2 \left(1 - \frac{V^*}{V(t)}\right) {}_0^C D_t^q V(t) + x_3 \left(1 - \frac{E^*}{E(t)}\right) {}_0^C D_t^q E(t) \\
&\quad + x_4 \left(1 - \frac{I^*}{I(t)}\right) {}_0^C D_t^q I(t) + x_5 \left(1 - \frac{Q^*}{Q(t)}\right) {}_0^C D_t^q Q(t) + x_6 \left(1 - \frac{R^*}{R(t)}\right) {}_0^C D_t^q R(t) \\
&= x_1 \left(1 - \frac{S^*}{S(t)}\right) (\Lambda - \alpha_1 S(t)I(t) - \delta S(t) - \mu S(t)) + x_2 \left(1 - \frac{V^*}{V(t)}\right) (\delta S(t) - \alpha_2 V(t)I(t) - \mu V(t)) \\
&\quad + x_3 \left(1 - \frac{E^*}{E(t)}\right) (\alpha_1 S(t)I(t) + \alpha_2 V(t)I(t) + \alpha_3 R(t)I(t) - \gamma E(t) - \mu E(t)) \\
&\quad + x_4 \left(1 - \frac{I^*}{I(t)}\right) (\gamma E(t) - \beta I(t) - \mu I(t)) + x_5 \left(1 - \frac{Q^*}{Q(t)}\right) (\beta I(t) - \lambda Q(t) - \kappa Q(t) - \mu Q(t)) \\
&\quad + x_6 \left(1 - \frac{R^*}{R(t)}\right) (\lambda Q(t) - \alpha_3 R(t)I(t) - \mu R(t)).
\end{aligned}$$

By the first expression of (17), we have

$$\begin{aligned}
{}_0^C D_t^q L_2(t) &\leq x_1 \left(1 - \frac{S^*}{S(t)}\right) (\alpha_1 S^* I^* + \delta S^* + \mu S^* - \alpha_1 S(t)I(t) - \delta S(t) - \mu S(t)) + x_2 \left(1 - \frac{V^*}{V(t)}\right) (\delta S(t) \\
&\quad - \alpha_2 V(t)I(t) - \mu V(t)) + x_3 \left(1 - \frac{E^*}{E(t)}\right) (\alpha_1 S(t)I(t) + \alpha_2 V(t)I(t) + \alpha_3 R(t)I(t) - \gamma E(t) - \mu E(t)) \\
&\quad + x_4 \left(1 - \frac{I^*}{I(t)}\right) (\gamma E(t) - \beta I(t) - \mu I(t)) + x_5 \left(1 - \frac{Q^*}{Q(t)}\right) (\beta I(t) - \lambda Q(t) - \kappa Q(t) - \mu Q(t)) \\
&\quad + x_6 \left(1 - \frac{R^*}{R(t)}\right) (\lambda Q(t) - \alpha_3 R(t)I(t) - \mu R(t)).
\end{aligned}$$

Then, it reads

$$\begin{aligned}
&{}_0^C D_t^q L_2(t) \\
&\leq x_1 \frac{\mu + \delta}{S(t)} (S(t) - S^*)^2 - (x_1 \alpha_1 S(t)I(t) + x_1 \alpha_1 S^* I(t) + x_2 (\delta S(t) - \alpha_2 V(t)I(t) - \mu V(t)) + x_3 (\alpha_1 S(t)I(t) \\
&\quad - (\gamma + \mu)E(t)) + x_4 (\gamma E(t) - (\beta + \mu)I(t)) + x_5 (\beta I(t) - (\lambda + \kappa + \mu)Q(t)) + x_6 (\lambda Q(t) - \alpha_3 R(t)I(t) \\
&\quad - \mu R(t)) + x_1 \alpha_1 S^* I^* + x_2 (\alpha_2 I(t) + \mu)V^* + x_3 \alpha_2 V(t)I(t) + x_3 \alpha_3 R(t)I(t) + x_3 (\gamma + \mu)E^* \\
&\quad + x_4 (\beta + \mu)I^* + x_5 (\lambda + \kappa + \mu)Q^* + x_6 (\alpha_3 I(t) + \mu)R^* - (x_1 \frac{S^*}{S(t)} \alpha_1 S^* I^* + x_2 \frac{V^*}{V(t)} \delta S(t) \\
&\quad + x_3 \frac{E^*}{E(t)} (\alpha_1 S(t)I(t) + \alpha_2 V(t)I(t) + \alpha_3 R(t)I(t)) + x_4 \frac{I^*}{I(t)} \gamma E(t) + x_5 \frac{Q^*}{Q(t)} \beta I(t) + x_6 \frac{R^*}{R(t)} \lambda Q(t)).
\end{aligned}$$

To eliminate the uncertainties, we let

$$x_1 = 1, x_2 = 1, x_3 = 1, x_4 = \frac{\gamma + \mu}{\gamma}, x_5 = \frac{(\gamma + \mu)(\beta + \mu)}{\gamma\beta}, x_6 = 1. \quad (18)$$

The following facts are used:

$$\begin{aligned}
I^* &= \frac{\lambda + \kappa + \mu}{\beta} Q^*, S^* = \frac{\alpha_2 I^* + \mu}{\delta} V^*, \mu R^* = \lambda Q^* + \alpha_3 R^* I^*, (\gamma + \mu)E^* = \alpha_1 S^* I^* + \alpha_2 V^* I^* + \alpha_3 R^* I^*, \\
\frac{(\gamma + \mu)(\beta + \mu)}{\gamma} I(t) \frac{Q^*}{Q(t)} &= \frac{(\gamma + \mu)(\beta + \mu)}{\gamma} I^* \frac{I(t)}{I^*} \frac{Q^*}{Q(t)}.
\end{aligned}$$

Then, after some rigorous arrangement, we arrive at

$$\begin{aligned}
{}_0^C D_t^q L_2(t) &\leq -\frac{\alpha_1 I(t) + \delta + \mu}{S(t)} (S(t) - S^*)^2 + \mu V^* \left(2 - \frac{V^*}{V(t)} - \frac{V(t)}{V^*}\right) \\
&\quad + (\alpha_1 S^* I^* + \alpha_2 V^* I^* + \alpha_3 R^* I^*) \left(2 - \frac{E^*}{E(t)} - \frac{E(t)}{E^*}\right) \\
&\quad + \frac{(\gamma + \mu)(\beta + \mu)I^*}{\gamma} \left(2 - \frac{I(t)}{I^*} \frac{Q^*}{Q(t)} - \frac{I^*}{I(t)} \frac{Q(t)}{Q^*}\right) + \lambda Q^* \left(2 - \frac{R^*}{R(t)} - \frac{R(t)}{R^*}\right).
\end{aligned}$$

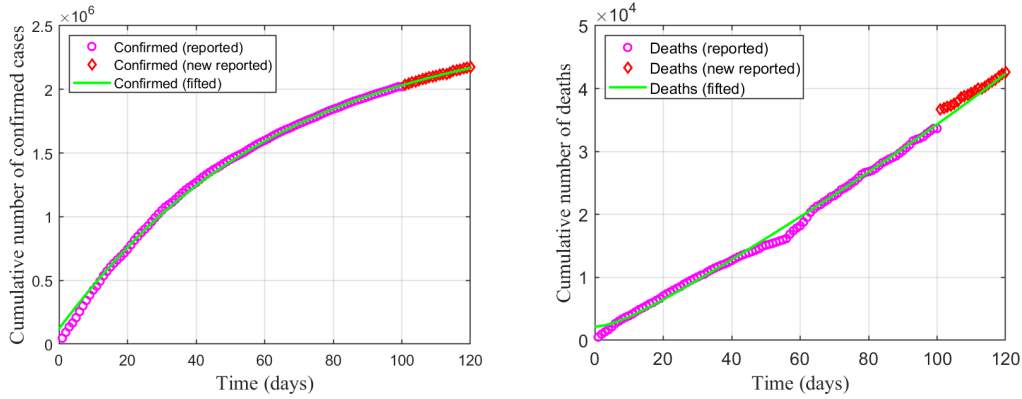


**Figure 2** Forecast of COVID-19 epidemics in India (the purple circles represent the real data fitting; the red diamonds is the real data for the 10-day forecast; the solid green lines represent fitting curves)

**Table 2** Identified parameters by least squares fitting for model (5).

Parameters	Value	Parameters	Value
$\Lambda$	770.96	$\alpha_1$	2.1003e-09
$\alpha_2$	1.0319e-10	$\alpha_3$	2.2153e-09
$\gamma$	0.0061	$\delta$	0.2162
$\beta$	0.0044	$\lambda$	0.1213
$\kappa$	0.0011	$\mu$	9.5787e-06
$q$	0.9647		

By considering equation (14) we can get that if  $R_0 > 1$ , then  ${}_0^C D_t^q L_2(t) \leq 0$ . The equality holds if and only if  $S(t) = S^*$ ,  $V(t) = V^*$ ,  $E(t) = E^*$ ,  $I(t) = I^*$ ,  $Q(t) = Q^*$  and  $R(t) = R^*$ . Thus, the only invariant set contained in  $\mathbb{R}_+^6$  is  $\{(S^*, V^*, E^*, I^*, Q^*, R^*)\}$ . Now, by the Lemma 4.6 of reference<sup>34</sup> implies that all solutions converge to the endemic equilibrium  $P_E$ . Therefore, the  $P_E$  of system (7) is globally asymptotically stable if  $R_0 > 1$ . This concludes the proof.

## 5 | NUMERICAL RESULTS

In this part, the real data of COVID-19 is from the Johns Hopkins University Center for Systems Science and Engineering (<https://github.com/CSSEGISandData/COVID-19>). The data includes accumulated confirmed cases and death cases worldwide.

The parameters in the model (5) are retrieved by solving the proposed inverse problem using data related to the number of infected and death individuals in India, from 27th August 2021 and 24th December 2021. The parameters in the model (5) are identified by fractional Adams-Bashforth-Moulton method and nonlinear least squares. The parameter values are given in Table 2, which can be used to fit the real data well in Figure 2. These parameters are also used to simulate the stability of equilibrium points, optimal control problems, and the impacts of vaccination and non-pharmaceutical interventions of the epidemic.

### 5.1 | Sensitivity analysis

Sensitivity analysis is a strong tool to assess the impact of each parameter on the spread of the disease. In order to rank the factors that influence the spread of COVID-19, we analyze the sensitivity analysis of model (7).

**Table 3** Sensitivity indexes of the basic reproduction number  $R_0$  for relevant parameters of model (7).

Parameters	Sensitivity Index	Sensitivity Value
$\Lambda$	$S_\Lambda$	1
$\beta$	$S_\beta$	-0.9978
$\alpha_1$	$S_{\alpha_1}$	9.0091e-04
$\delta$	$S_\delta$	-8.5661e-04
$\gamma$	$S_\gamma$	0.0016
$\alpha_2$	$S_{\alpha_2}$	0.9991

From (11), it can be seen that the basic reproduction number  $R_0$  depends on the parameters  $\gamma, \Lambda, \beta, \delta, \alpha_1, \alpha_2$  and  $\mu$ . The relationships between the parameters and  $R_0$  are shown below:  $\frac{\partial R_0}{\partial \gamma} > 0, \frac{\partial R_0}{\partial \Lambda} > 0, \frac{\partial R_0}{\partial \beta} < 0, \frac{\partial R_0}{\partial \delta} < 0, \frac{\partial R_0}{\partial \alpha_1} > 0, \frac{\partial R_0}{\partial \alpha_2} > 0, \frac{\partial R_0}{\partial \mu} < 0$ . It is obvious that  $\gamma, \Lambda, \alpha_1$ , and  $\alpha_2$  are positively correlated with  $R_0$ , while  $\beta, \delta$  and  $\mu$  are negatively correlated with  $R_0$ .

In order to accurately characterize the relationships between the parameters and  $R_0$ , the direct differentiation method<sup>7</sup> is used to calculate the sensitivity index. The result not only gives the factors that influence the spread of the disease, but also provides quantitative information between the parameters related to  $R_0$ . The following formula is adopted to calculate the sensitivity index of the  $R_0$  in the model (7):

$$S_\Phi = \frac{\Phi}{R_0} \frac{\partial R_0}{\partial \Phi}, \quad (19)$$

where  $\Phi$  is a parameter in the  $R_0$ .

From Table 3, the parameters  $\Lambda, \alpha_1, \gamma$  and  $\alpha_2$  have positive effect on the  $R_0$ , which manifest that the increase or decrease of these parameters say by 10% can growth or decay the  $R_0$  by 10%, 0.009%, 0.016% and 9.991%, respectively.

Beside that, the increase of the parameters  $\beta$  and  $\delta$  10% can decay the  $R_0$  by 9.978% and 0.008%, respectively. Furthermore, we have  $|S_\Lambda| > |S_{\alpha_2}| > |S_\beta|$ , which indicates that  $\alpha_2$  and  $\beta$  are the most influential parameters to reduce  $R_0$ . That is the most effective way to prevent COVID-19 spread is to accelerate isolation speed and reduce vaccine inefficacy rates.

## 5.2 | Numerical simulation of the stability analysis

In this subsection, some numerical results of model (7) are presented to verify the stability of equilibrium points given by the Theorems 3 and 4.

From Table 2 and equation (11), it is obvious that  $R_0 = 1.89 > 1$ . Figure 3 shows that a state trajectory converges to the endemic equilibrium point  $P_E(2.51 \times 10^3, 1.19 \times 10^5, 9.78 \times 10^6, 1.36 \times 10^7, 4.87 \times 10^5, 1.96 \times 10^6)$ . Therefore, the numerical result is consistent with the theoretical result when the  $R_0$  exceeds unity. It means that COVID-19 is not eradicated under the same prevention and control measures, and therefore warns the people to maintain suitable safety measures.

To verify that the disease-free equilibrium point  $P_F$  of model (7) is asymptotically stable when  $R_0 < 1$ , we let  $\alpha_1 = 2.1003e-10, \alpha_2 = 2.0319e-11, \alpha_3 = 2.2153e-10, \beta = 0.0094, \gamma = 0.0001, \delta = 0.8162, \kappa = 0.0011$ , and the other parameters are the same as Table 2. By (11), we have  $R_0 = 0.15$ , that is the  $R_0$  is less than one. From Figure 4, it can be clearly seen that the solution of model (7) converges to  $P_F(9.45 \times 10^2, 8.05 \times 10^7, 0, 0, 0, 0)$ . Furthermore, we find that the stability results obtained numerically for fractional model (7) do coincide with theoretical results.

In the face of COVID-19 variant, some of the most widely used vaccines have faltered. Figure 5 shows the impact of different vaccine inefficacy rates on the disease transmission. In detail, when the vaccine inefficacy  $\alpha_2 = 1.6987e-10$ , the number of people protected by the vaccine decreases about 10 times, and the number of death individuals increases about 3 times. This indicates that the rate of vaccine protection has an important impact on the spread of the disease.

As the virus continues to mutate, it is now clear that COVID-19 reinfections are very common. Figure 6 shows the impact of different reinfection rates on the disease transmission. We find that when different reinfection rate  $\alpha_3$  increased from 0 to  $5.1595e-10$ , the total number of infected cases  $E + I + Q$  increased by about 2 times and the number of recovered individuals decreased by about 4 times, that is the population is more likely to be infected by the virus. The result shows if the mutated virus has a strong ability to reinfect, the risk of infection in healthy peoples will increase dramatically.

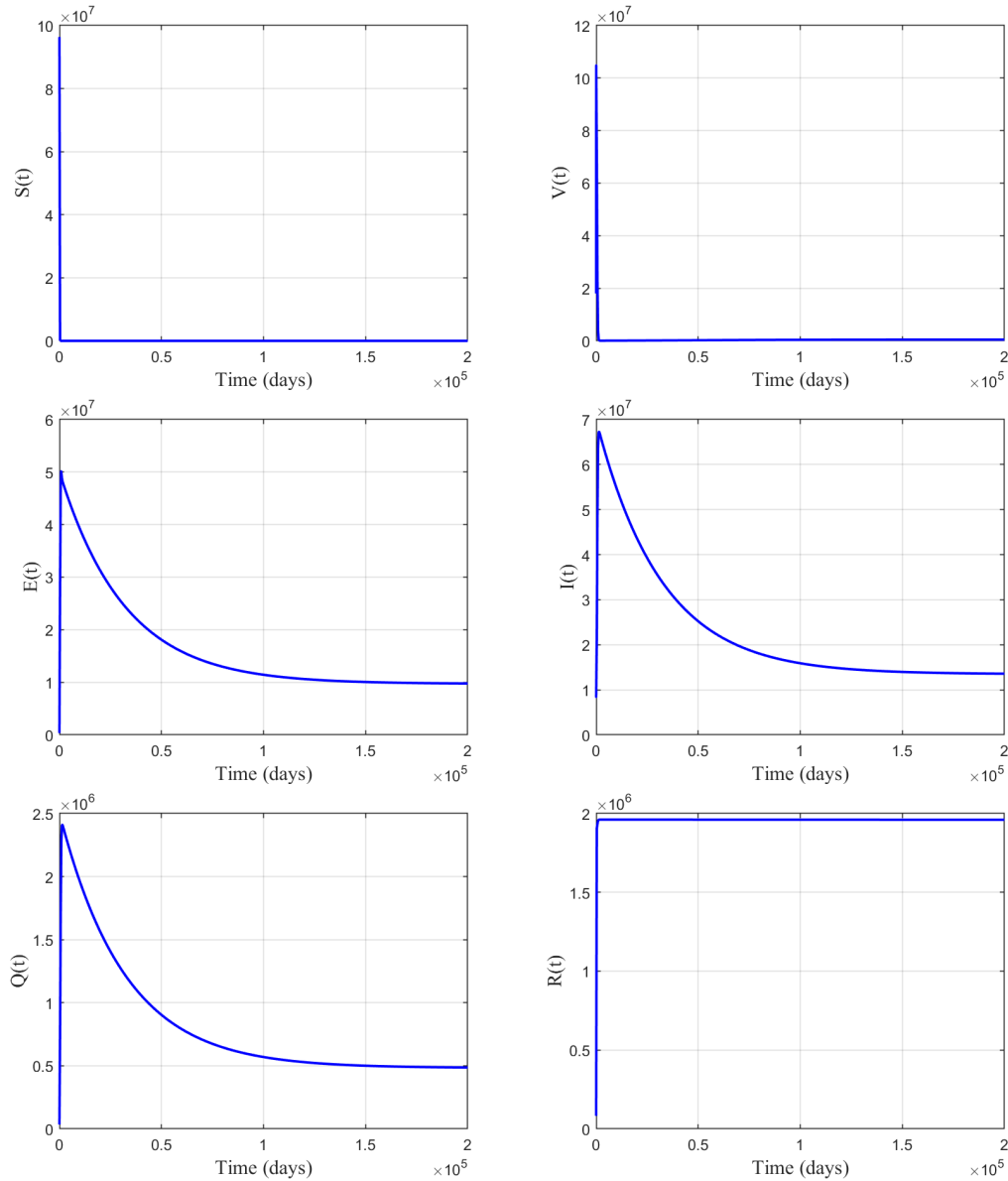


**Figure 3** Stability of model (7) around the endemic equilibrium  $P_E$

## 6 | OPTIMAL CONTROL STRATEGY

In this part, we analyze the necessary conditions for implementing optimal control and derive the corresponding optimal solution by the Pontryagin's maximum principle.<sup>35</sup>

There are many different control strategies to prevent the disease transmission. Non-pharmaceutical interventions is one of the effective precautionary measures which is suggested to be obeyed by everyone. Besides that, people are urged to get vaccinated to avoid infection. So, two strategies are incorporated into model (7) to reduce the number of deaths and infected people.

Non-pharmaceutical interventions and vaccination are chosen as control strategies, which are added to model (7). We consider that  $u_1(t)$  portion of the susceptible individuals take non-pharmaceutical interventions, such as maintaining social distancing and using the face masks. Thus, only  $(1 - u_1(t))S$  of susceptible individuals move to the exposure stage. Furthermore, instead of constant vaccination rate, time-dependent rate  $u_2(t)$  is considered in model (7). Therefore, the model (7) can be rewritten as

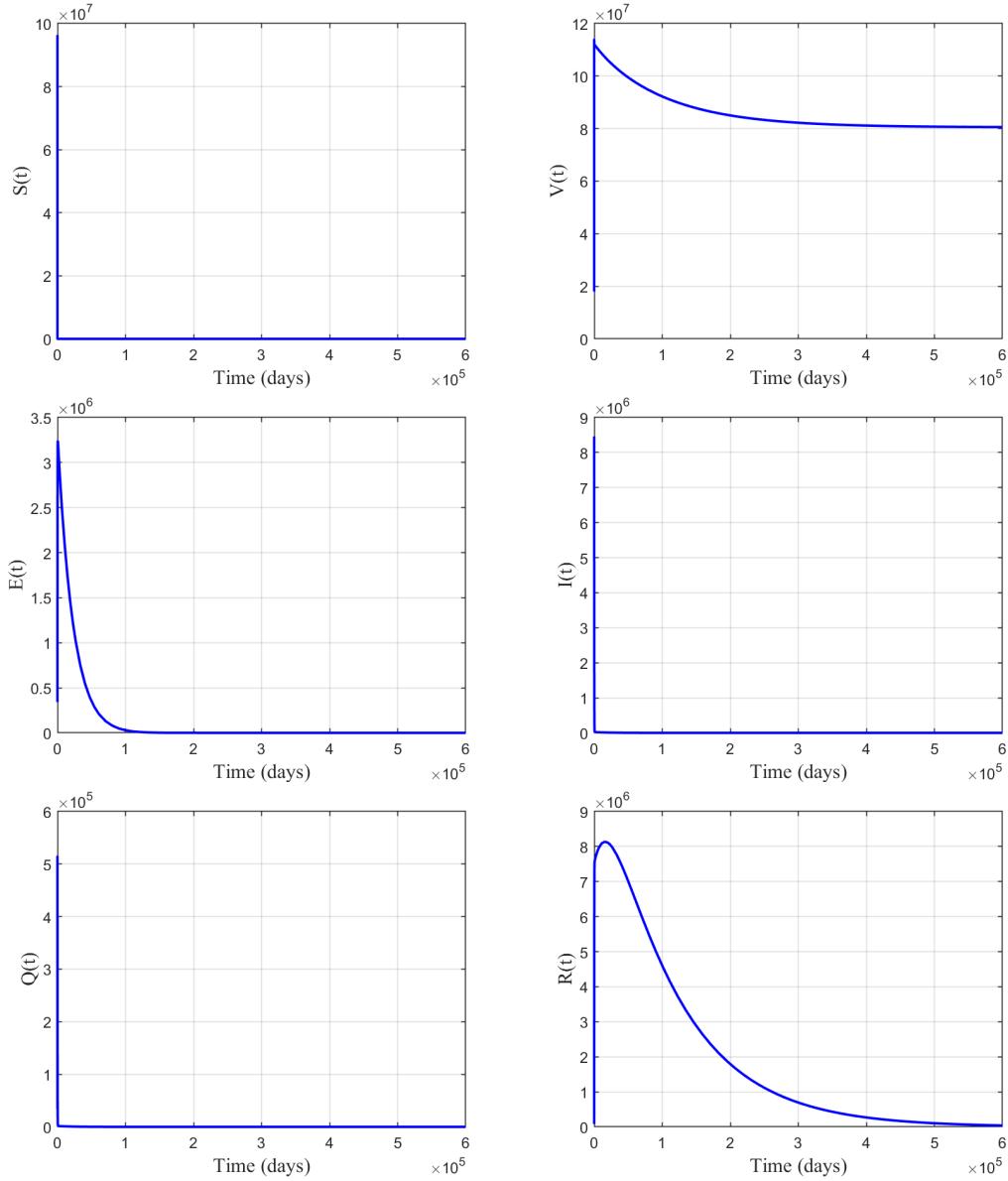


**Figure 4** Stability of model (7) around the disease-free equilibrium  $P_F$

$$\begin{aligned}
 {}_0^C D_t^q S(t) &= \Lambda - \alpha_1(1 - u_1(t))S(t)I(t) - u_2(t)S(t) - \mu S(t), \\
 {}_0^C D_t^q V(t) &= u_2(t)S(t) - \alpha_2 V(t)I(t) - \mu V(t), \\
 {}_0^C D_t^q E(t) &= \alpha_1(1 - u_1(t))S(t)I(t) + \alpha_2 V(t)I(t) + \alpha_3 R(t)I(t) - \gamma E(t) - \mu E(t), \\
 {}_0^C D_t^q I(t) &= \gamma E(t) - \beta I(t) - \mu I(t), \\
 {}_0^C D_t^q Q(t) &= \beta I(t) - \lambda Q(t) - \kappa Q(t) - \mu Q(t), \\
 {}_0^C D_t^q R(t) &= \lambda Q(t) - \alpha_3 R(t)I(t) - \mu R(t), \\
 {}_0^C D_t^q D(t) &= \kappa Q(t),
 \end{aligned} \tag{20}$$

with initial conditions

$$S(t_0) \geq 0, V(t_0) \geq 0, E(t_0) \geq 0, I(t_0) \geq 0, Q(t_0) \geq 0, R(t_0) \geq 0, D(t_0) \geq 0.$$

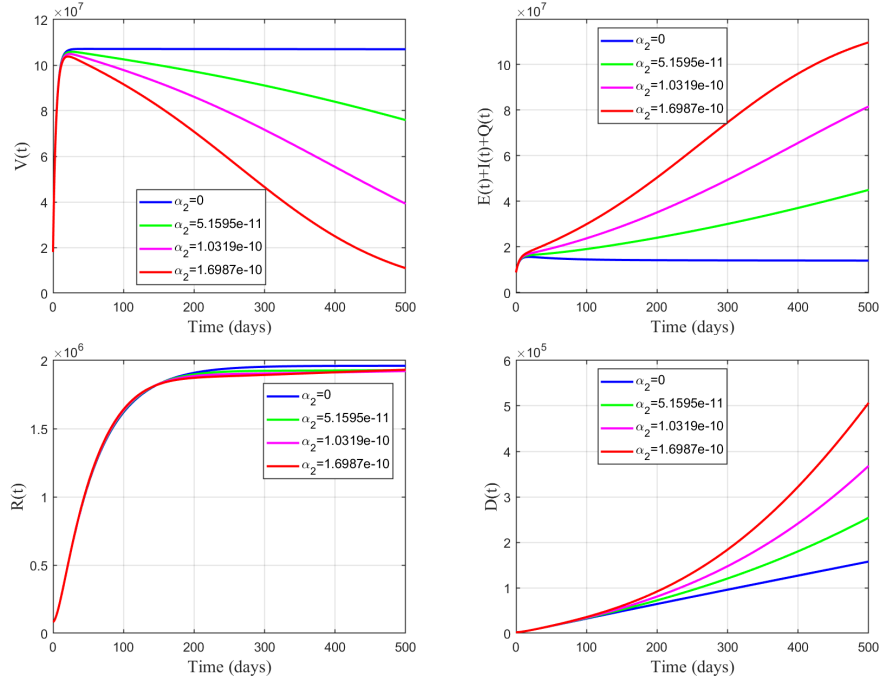


**Figure 5** The impact of different vaccine inefficiency rates on the spread of the epidemic

The objective function  $J(u_1, u_2)$  of fractional dynamical system (20) is given by

$$J(u_1, u_2) = \frac{1}{\Gamma(n-q)} \int_0^T (T-\tau)^{n-q-1} (a_1 Q(\tau) + a_2 D(\tau) + \frac{1}{2} b_1 u_1^2(\tau) + \frac{1}{2} b_2 u_2^2(\tau)) d\tau, \quad (21)$$

where  $a_1 \in \mathbb{R}^+$  and  $a_2 \in \mathbb{R}^+$  are introduced to maintain a balance between  $Q$  and  $D$ , and  $T$  is the final control time. Moreover,  $b_1$  and  $b_2$  represent the proportional weights of the costs  $u_1$  and  $u_2$ , respectively.

Let  $\Psi = \{(u_1(t), u_2(t)) : 0 \leq u_1 \leq u_{1max} \leq 1, 0 \leq u_2 \leq u_{2max} \leq 1, t \in [0, T]\}$  be a set of admissible control functions and Lebesgue measurable. When  $u_i = 0$  shows that the control strategy is invalid, while  $u_i = 1$  means that the control strategy is completely implemented.

**Theorem 7.** If the optimal controls  $u_1^*$  and  $u_2^*$  and corresponding optimal states  $(S^*, V^*, E^*, I^*, Q^*, R^*, D^*)$  exist for system (20), then we have adjoint variables  $p_i, i = 1, 2, \dots, 7$  satisfy the following equations:

$$\begin{aligned} {}_0^C D_t^q p_1(T-t) &= \alpha_1 (p_3(T-t) - p_1(T-t)) I^*(T-t) (1 - u_1^*(T-t)) + u_2^*(T-t) (p_2(T-t) \\ &\quad - p_1(T-t)) - \mu p_1(T-t), \\ {}_0^C D_t^q p_2(T-t) &= \alpha_2 (p_3(T-t) - p_2(T-t)) I^*(T-t) - \mu p_2(T-t), \\ {}_0^C D_t^q p_3(T-t) &= \gamma (p_4(T-t) - p_3(T-t)) - \mu p_3(T-t), \\ {}_0^C D_t^q p_4(T-t) &= \alpha_1 (p_3(T-t) - p_1(T-t)) (1 - u_1^*(T-t)) S^*(T-t) + \alpha_2 (p_3(T-t) - p_2(T-t)) V^*(T-t) \\ &\quad + \alpha_3 (p_3(T-t) - p_6(T-t)) R^*(T-t) + \beta (p_5(T-t) - p_4(T-t)) - \mu p_4(T-t), \\ {}_0^C D_t^q p_5(T-t) &= a_1 - (\lambda + \kappa + \mu) p_5(T-t) + \lambda p_6(T-t) + \kappa p_7(T-t), \\ {}_0^C D_t^q p_6(T-t) &= \alpha_3 (p_3(T-t) - p_6(T-t)) I^*(T-t) - \mu p_6(T-t), \\ {}_0^C D_t^q p_7(T-t) &= a_2, \end{aligned}$$

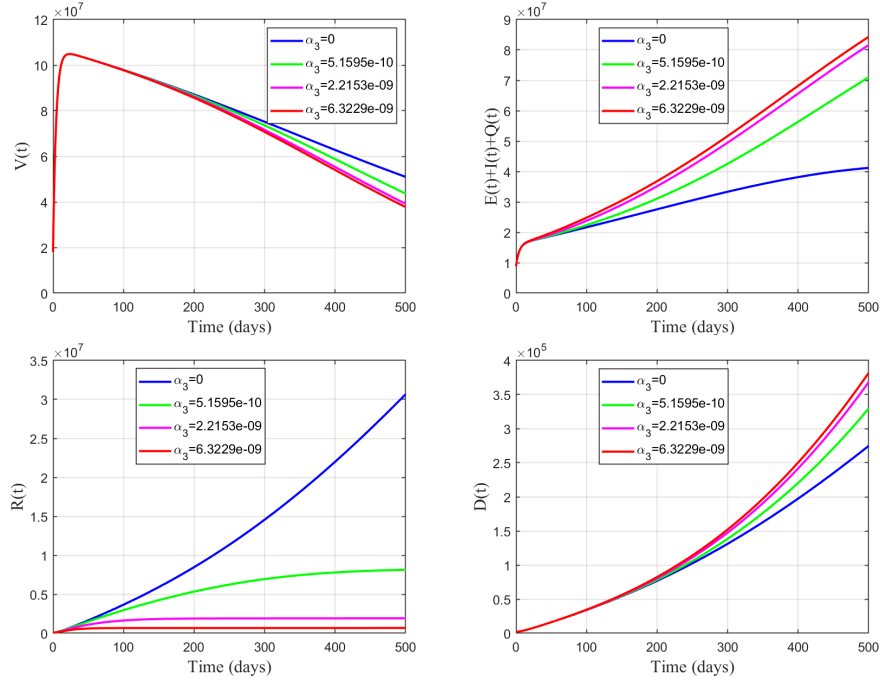


**Figure 6** The impact of different reinfection rates on the spread of the epidemic

with transversally conditions  $p_i(T) = 0$ ,  $i = 1, 2, \dots, 7$ , on the set  $\Psi$ . Furthermore, the optimal controls  $u_1^*$  and  $u_2^*$  are given by

$$u_1^* = \min \left\{ \mu_{1 \max}, \max \left( \frac{\alpha_1(p_3 - p_1)S^*I^*}{b_1} \right) \right\},$$

$$u_2^* = \min \left\{ \mu_{2 \max}, \max \left( \frac{(p_1 - p_2)S^*}{b_2} \right) \right\}.$$

**proof.** To minimize the objective function (21), the Hamiltonian is designed as follows,

$$\begin{aligned} H(S, V, E, I, Q, R, D, p_i, u_1, u_2) = & a_1 Q(t) + a_2 D(t) + \frac{1}{2} b_1 u_1^2(t) + \frac{1}{2} b_2 u_2^2(t) \\ & + p_1 (\Lambda - \alpha_1 (1 - u_1(t)) S(t) I(t) - u_2(t) S(t) - \mu S(t)) \\ & + p_2 (u_2(t) S(t) - \alpha_2 V(t) I(t) - \mu V(t)) \\ & + p_3 (\alpha_1 (1 - u_1(t)) S(t) I(t) + \alpha_2 V(t) I(t) + \alpha_3 R(t) I(t)) \\ & - \gamma E(t) - \mu E(t) + p_4 (\gamma E(t) - \beta I(t) - \mu I(t)) + p_5 (\beta I(t) - \lambda Q(t)) \\ & - \kappa Q(t) - \mu Q(t) + p_6 (\lambda Q(t) - \alpha_3 R(t) I(t) - \mu R(t)) + p_7 \kappa Q(t). \end{aligned}$$

With the help of the Pontryagin's maximum principle, the adjoint variables are obtained by solving the below adjoint equations

$$\begin{aligned}
{}_i D_T^q p_1 &= \frac{\partial H}{\partial S} = \alpha_1(p_3 - p_1)(1 - u_1^*)I^* + u_2^*(p_2 - p_1) - \mu p_1, \\
{}_i D_T^q p_2 &= \frac{\partial H}{\partial V} = \alpha_2(p_3 - p_2)I^* - \mu p_2, \\
{}_i D_T^q p_3 &= \frac{\partial H}{\partial E} = \gamma(p_4 - p_3) - \mu p_3, \\
{}_i D_T^q p_4 &= \frac{\partial H}{\partial I} = \alpha_1(p_3 - p_1)(1 - u_1^*)S^* + \alpha_2(p_3 - p_2)V^* + \alpha_3(p_3 - p_6)R^* + \beta(p_5 - p_4) - \mu p_4, \\
{}_i D_T^q p_5 &= \frac{\partial H}{\partial Q} = a_1 - (\lambda + \kappa + \mu)p_5 + \lambda p_6 + \kappa p_7, \\
{}_i D_T^q p_6 &= \frac{\partial H}{\partial R} = \alpha_3(p_3 - p_6)I^* - p_6 \mu, \\
{}_i D_T^q p_7 &= \frac{\partial H}{\partial D} = a_2,
\end{aligned}$$

with the transversality conditions  $p_i(T) = 0$ ,  $i = 1, 2, \dots, 7$ , where  ${}_i D_T^q$  is the right Riemann-Liouville fractional derivative.

It is worth noting that the adjoint variables are given by the right Riemann-Liouville fractional derivative. According to lemma 3, we can get the adjoint variables with the right Caputo fractional derivative as follows

$$\begin{aligned}
{}_i^C D_T^q p_1(t) &= \alpha_1 (p_3(t) - p_1(t)) I^*(t)(1 - u_1^*(t)) + u_2^*(t)(p_2(t) - p_1(t)) - \mu p_1(t), \\
{}_i^C D_T^q p_2(t) &= \alpha_2 (p_3(t) - p_2(t)) I^*(t) - \mu p_2(t), \\
{}_i^C D_T^q p_3(t) &= \gamma(p_4(t) - p_3(t)) - \mu p_3(t), \\
{}_i^C D_T^q p_4(t) &= \alpha_1(p_3(t) - p_1(t))(1 - u_1^*)S^*(t) + \alpha_2(p_3(t) - p_2(t))V^*(t) \\
&\quad + \alpha_3(p_3(t) - p_6(t))R^*(t) + \beta(p_5(t) - p_4(t)) - \mu p_4(t), \\
{}_i^C D_T^q p_5(t) &= a_1 - (\lambda + \kappa + \mu)p_5(t) + \lambda p_6(t) + \kappa p_7(t), \\
{}_i^C D_T^q p_6(t) &= \alpha_3(p_3(t) - p_6(t))I^*(t) - \mu p_6(t), \\
{}_i^C D_T^q p_7(t) &= a_2.
\end{aligned} \tag{22}$$

According to Lemma 15 of reference<sup>31</sup>, the system (22) is transformed into the following system:

$$\begin{aligned}
{}_0^C D_t^q p_1(T-t) &= \alpha_1(p_3(T-t) - p_1(T-t))(1 - u_1)I(T-t) + u_2(p_2(T-t) - p_1(T-t)) - \mu p_1(T-t), \\
{}_0^C D_t^q p_2(T-t) &= \alpha_2(p_3(T-t) - p_2(T-t))I(T-t) - \mu p_2(T-t), \\
{}_0^C D_t^q p_3(T-t) &= \gamma(p_4(T-t) - p_3(T-t)) - \mu p_3(T-t), \\
{}_0^C D_t^q p_4(T-t) &= \alpha_1(p_3(T-t) - p_1(T-t))(1 - u_1)S(T-t) + \alpha_2(p_3(T-t) - p_2(T-t))V(T-t) \\
&\quad + \alpha_3(p_3(T-t) - p_6(T-t))R(T-t) + \beta(p_5(T-t) - p_4(T-t)) - \mu p_4(T-t), \\
{}_0^C D_t^q p_5(T-t) &= a_1 - (\lambda + \kappa + \mu)p_5(T-t) + \lambda p_6(T-t) + \kappa p_7(T-t), \\
{}_0^C D_t^q p_6(T-t) &= \alpha_3(p_3(T-t) - p_6(T-t))I - p_6(T-t)\mu, \\
{}_0^C D_t^q p_7(T-t) &= a_2,
\end{aligned}$$

with the transversality conditions  $p_i(T) = 0$ ,  $i = 1, 2, \dots, 7$ . From optimality conditions  $\frac{\partial H}{\partial \mu_i(t)} = 0$ ,  $i = 1, 2$ , the optimal control parameters  $u_1^*$  and  $u_2^*$  are obtained by solving the following system:

$$\begin{aligned}
\frac{\partial H}{\partial u_1(t)} \Big|_{u_1(t)=u_1^*} &= b_1 u_1^* + \alpha_1(p_1 - p_3)S^* I^* = 0, \\
\frac{\partial H}{\partial u_2(t)} \Big|_{u_1(t)=u_2^*} &= b_2 u_2^* + (p_2 - p_1)S^* = 0.
\end{aligned}$$

Therefore, we obtain

$$u_1^* = \frac{\alpha_1(p_3 - p_1)S^* I^*}{b_1}, \quad u_2^* = \frac{(p_1 - p_2)S^*}{b_2}. \tag{23}$$

Now from (23), along with the characteristics of control set  $\Psi$ , we have

$$u_1^* = \begin{cases} 0, & \text{if } \frac{\alpha_1(p_3-p_1)S^*I^*}{b_1} < 0, \\ \frac{\alpha_1(p_3-p_1)S^*I^*}{b_1}, & \text{if } 0 \leq \frac{\alpha_1(p_3-p_1)S^*I^*}{b_1} \leq 1, \\ 1, & \text{if } \frac{\alpha_1(p_3-p_1)S^*I^*}{b_1} > 1. \end{cases}$$

$$u_2^* = \begin{cases} 0, & \text{if } \frac{(p_1-p_2)S^*}{b_2} < 0, \\ \frac{\alpha_1(p_1-p_2)S^*I^*}{b_1}, & \text{if } 0 \leq \frac{(p_1-p_2)S^*}{b_2} \leq 1, \\ 1, & \text{if } \frac{(p_1-p_2)S^*}{b_2} > 1. \end{cases}$$

This complete the proof.

Three control strategies are shown in Table 4 which illustrates the impact of different control strategies on the spread of the disease. It can be seen from Table 4 that the non-pharmaceutical interventions  $u_1$  can reduce the number of infected cases by 52% and deaths by 56%, and the vaccination  $u_2$  can reduce the number of infected cases by 77% and deaths by 60%. In addition, the use of control strategies  $u_1$  and  $u_2$  together can reduce the number of infections and deaths by 80% and 61%, respectively. The results show that  $u_1, u_2$  are the best control strategies (see Figure 7) to minimize the number of infections and deaths, i.e. we need to combine non-pharmaceutical interventions with vaccination to prevent the spread of COVID-19. However, using vaccination  $u_2$  alone is only marginally different from using non-pharmaceutical interventions  $u_1$  and vaccination  $u_2$  together.

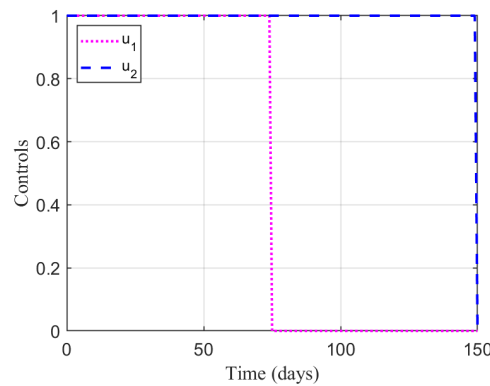


**Figure 7** When  $T=150$ , profile of optimal control  $u_1$  and  $u_2$

The effects of without control ( $u_1 = u_2 = 0$ ), weak control ( $u_1 = u_2 = 0.02$ ), medium control ( $u_1 = u_2 = 0.5$ ), optimal control and maximum control ( $u_1 = u_2 = 1$ ) on the spread of the disease are compared in Figure 8. Under the same economic cost, the optimal control strategy can produce more control benefits than the weak control and medium control strategies. In addition, we get control costs of no control, weak control, medium control, optimal control and maximum control, as shown in Figure 9. Obviously, optimal control achieves the best control effect by minimizing the control cost.

As can be seen from Table 5, the higher the maximum control intensity of non-pharmaceutical interventions, the greater the reduction in the number of infections and deaths, and the lower the cost of control. Similarly, when the maximum control intensity of vaccination increase, it dramatically reduces the number of infections, deaths and control costs. Therefore, increasing the maximum intensity of control can effectively reduce the number of infections, deaths and control costs.

Figure 10 shows that non-pharmaceutical interventions reduce the number of infected humans and deaths at a higher rate than vaccination measure over shorter control periods, but the effect of vaccination measure become more pronounced as control periods increased. Thus, vaccination is a more effective treatment for COVID-19 in the long term.

Virus variations generally lead to change in the rates of infection, vaccine inefficacy and reinfection. We consider three types of variation intensity, namely weak ( $\bar{\alpha}_1 = 1.8\alpha_1, \bar{\alpha}_2 = 1.8\alpha_2, \bar{\alpha}_3 = 1.8\alpha_3$ ), medium ( $\bar{\alpha}_1 = 4.2\alpha_1, \bar{\alpha}_2 = 4.2\alpha_2, \bar{\alpha}_3 = 4.2\alpha_3$ ) and strong ( $\hat{\alpha}_1 = 7.5\alpha_1, \hat{\alpha}_2 = 7.5\alpha_2, \hat{\alpha}_3 = 7.5\alpha_3$ ) variations. Table 6 shows the influence of different degrees of variation on disease

**Table 4** When  $T = 150$ , reduced percentages of the number of infectious and death individuals with different control strategies.

	Strategies	Percentage (%)
Infectious	$u_1$	52.3149
	$u_2$	76.5427
	$u_1, u_2$	79.0235
Death	$u_1$	56.4144
	$u_2$	59.2121
	$u_1, u_2$	61.4818

**Table 5** Reduced percentages of different maximum control intensities on infections and deaths, and the corresponding control costs  $J_u$ .

	Max-value	Infectious (%)	Death (%)	$J_u$
$u_{1max}$	0.15	3.3302	5.2158	4.2440e+09
	0.35	9.2308	13.6745	3.8607e+09
	0.55	17.4834	24.1693	3.3869e+09
	0.75	29.2539	36.9800	2.8103e+09
	0.95	46.6550	52.2294	2.1262e+09
$u_{2max}$	0.15	67.3252	50.2939	2.2264e+09
	0.35	73.2971	55.9963	1.9679e+09
	0.55	75.0877	57.7638	1.8875e+09
	0.75	75.9480	58.6204	1.8486e+09
	0.95	76.4492	59.1195	1.8259e+09

**Table 6** Reduced percentages of the number of infected humans and deaths by different degrees of virus variation

	Strategies	Weak (%)	Medium (%)	Strong (%)
Infectious	$u_1$	31.2628	21.5023	15.4241
	$u_2$	71.1597	53.7875	36.2916
	$u_1, u_2$	74.9841	61.0761	44.5068
Death	$u_1$	46.6359	39.1491	31.3551
	$u_2$	59.8926	53.7075	43.5065
	$u_1, u_2$	63.7576	59.7492	51.4675

transmission under with the above optimal control strategy  $u_1$  and  $u_2$ . It is obvious that when the variation intensity increases, the effect of the optimal control strategy will be weakened. That means we need to develop new vaccines when the intensity of the mutation increases.

## 7 | DISCUSSION AND CONCLUSIONS

In this paper, a new fractional model is constructed for mutated COVID-19 pandemic. The model formulation is studied in detail with the occurring of reinfection and vaccine inefficacy. After formulation of the model, the positivity and boundedness of the solution are estimated. The basic reproduction number  $R_0$  is given by

$$R_0 = \frac{\gamma \Lambda (\alpha_1 \mu + \alpha_2 \delta)}{\mu (\delta + \mu) (\gamma + \mu) (\beta + \mu)}.$$

When  $R_0 < 1$ , the disease-free equilibrium of the model is locally as well as globally asymptotically stable. Furthermore, when  $R_0 > 1$ , by constructing a suitable Lyapunov function, the endemic equilibrium is globally asymptotically stable.

From the real cumulative infection and death of COVID-19 in India, the model parameters are fitted by fractional Adams-Bashforth-Moulton method. Then, the basic reproduction number is  $R_0 = 1.89$ . Through a large number of numerical experiments, we propose the following advice to fight the mutated COVID-19 pandemic:

1. With a lot of real data, the state trajectory of the model converges to the endemic equilibrium point, that is COVID-19 will become endemic rather than extinct. Thus, we need to be prepared to live with COVID-19 for a long time under the current control strategy.
2. Recovering individuals who are reinfected have a greater impact on the spread of the disease. If the number of reinfected peoples are not quarantined, we may face a large number of new infected and dead cases. Therefore, identifying the reinfection cases and their isolations are beneficial to eradicate of the disease.
3. Stronger viral mutations can increase vaccine inefficacy rates, which can lead to an increase in the number of infections and deaths. Therefore, it is particularly important to develop new vaccines with higher protection rates if emerging viruses become more resistant to vaccines.
4. Compared with a combination of non-pharmaceutical interventions and vaccination strategy, the vaccine-only strategy has little difference in the number of infections and deaths.

## ACKNOWLEDGEMENTS

This work was supported by the Alianza UCMX Special Funding for Binational Collaboration Addressing COVID-19, the Natural Science Foundation of Gansu Province (No. 22JR5RA184), and the Innovation Team of Intelligent Computing and Dynamical System Analysis and Application of Northwest Minzu University.

## CONFLICT OF INTEREST

The authors have no competing interests.

## References

1. J. S. Lavine, O. N. Bjornstad and R. Antia, Immunological characteristics govern the transition of COVID-19 to endemicity, *Science* 371(6530) (2021) 741-745.
2. M. Nicola, Z. Alsafi, C. Sohrabi, A. Kerwan, et al., The socio-economic implications of the coronavirus pandemic (COVID-19), A review. *J. Surg. Res.* 78 (2020) 185-193.
3. E. Callaway and H. Ledford, How bad is Omicron? What scientists know so far, *Nature* 600(7888) (2021) 197-199.
4. V. J. Hall, S. Foulkes, A. Charlett, A. Atti, E. J. Monk, et al., SARS-CoV-2 infection rates of antibody-positive compared with antibody-negative health-care workers in England: a large, multicentre, prospective cohort study (SIREN), *Lancet* 397(10283) (2021) 1459-1469.

5. C. Watson, Three, four or more: what's the magic number for booster shots, *Nature* 602(7895) (2022) 17-18.
6. S. Y. Ren, W. B. Wang, R. D. Gao and A. M. Zhou, Omicron variant (B. 1.1. 529) of SARS-CoV-2: Mutation, infectivity, transmission, and vaccine resistance, *World J. Clin. Cases* 10(1) (2022) 1-11.
7. L. Peng, W. Yang, D. Zhang, C. Zhuge and L. Hong, Epidemic analysis of COVID-19 in China by dynamical modeling, *arXiv preprint arXiv:2002 (2020) 06563*. <https://doi.org/10.48550/arXiv.2002.06563>
8. T. Odagaki, Exact properties of SIQR model for COVID-19, *Physica A* 564 (2021) 125564.
9. B. Tang, X. Wang, Q. Li, N. L. Bragazzi, S. Tang, Y. Xiao and J. Wu, Estimation of the transmission risk of the 2019-nCoV and its implication for public health interventions, *J. Clin. Med* 9(2) (2020) 462-474 .
10. Z. Ma, S. Wang, X. Lin, X. Li, X. Han, H. Wang and H. Liu, Modeling for COVID-19 with the contacting distance, *Nonlinear Dyn* 107 (2022) 3065-3084.
11. C. Xu, Y. Yu, Y. Chen and Z. Lu, Forecast analysis of the epidemics trend of COVID-19 in the USA by a generalized fractional-order SEIR model, *Nonlinear Dyn* 101(3) (2020) 1621-1634.
12. W. Zhou, A. Wang, F. Xia, Y. Xiao and S. Tang, Effects of media reporting on mitigating spread of COVID-19 in the early phase of the outbreak, *Math Biosci Eng* 17(3) (2020) 2693-2707.
13. N. Ma, W. Ma and Z. Li, Multi-Model Selection and Analysis for COVID-19, *Fractal Fract* 5(3) (2021) 120.
14. Q. Zheng, X. Wang, C. Bao, Y. Ji, H. Liu, et al., A multi-regional, hierarchical tier mathematical model of the spread and control of COVID-19 epidemics from epicentre to adjacent regions, *Transbound Emerg Dis* 69(2) (2022) 549-558.
15. T. Sardar, S. Rana, S. Bhattacharya, K. Al-Khaled and J. Chattopadhyay, A generic model for a single strain mosquito-transmitted disease with memory on the host and the vector, *Math Biosci* 263 (2015) 18-36.
16. A. K. Singh, M. Mehra and S. Gulyani, A modified variable-order fractional SIR model to predict the spread of COVID-19 in India, *Math Meth Appl Sci* (2021)1-15. <https://doi.org/10.1002/mma.7655>.
17. Z. Lu, Y. Yu, Y. Chen, G. Ren, C. Xu, S. Wang and Z. Yin, A fractional-order SEIHDR model for COVID-19 with inter-city networked coupling effects, *Nonlinear Dyn* 101(3) (2020) 1717-1730.
18. D. Baleanu, M. H. Abadi, A. Jajarmi, K. Z. Vahid and J. J. Nieto, A new comparative study on the general fractional model of COVID-19 with isolation and quarantine effects, *Alex. Eng. J* 61(6) (2022) 4779-4791.
19. W. Ma, Y. Zhao, L. Guo and Y. Chen, Qualitative and quantitative analysis of the COVID-19 pandemic by a two-side fractional-order compartmental model, *ISA Trans* 124 (2022) 144-156.
20. M. A. A. Oud, A. Ali, H. Alrabaiah, S. Ullah, M. A. Khan, et al., A fractional order mathematical model for COVID-19 dynamics with quarantine, isolation, and environmental viral load, *Adv. Differ. Equ.* 2021(1) (2021) 1-19.
21. M. Khatun, M. Biswas and H. Ali, Mathematical analysis and optimal control applied to the treatment of leukemia, *J. Comput. Appl. Math* 64(1) (2020) 331-353.
22. L. Xue, X. Ren, F. Magpantay, W. Sun and H. Zhu, Optimal control of mitigation strategies for dengue virus transmission, *Bull. Math. Biol* 83(2) (2021) 1-28.
23. S. I. Oke, M. B. Matadi and S. S. Xulu, Optimal control analysis of a mathematical model for breast cancer, *J. Comput. Appl. Math* 23(2) (2018) 21.
24. Q. Zheng, X. Wang, Q. Pan and L. Wang, Optimal strategy for a dose-escalation vaccination against COVID-19 in refugee camps, *AIMS Mathematics* 7(5) (2022) 9288-9310.
25. S. Das, *Functional fractional calculus*, Berlin: Springer (2011)

26. P. A. Naik, J. Zu and K. M. Owolabi, Global dynamics of a fractional order model for the transmission of HIV epidemic with optimal control, *Chaos Solitons Fractals* 138 (2020) 109826.
27. A. Boukhouima, E. M. Lotfi, M. Mahrouf, S. Rosa, D. F. Torres, et al., Stability analysis and optimal control of a fractional HIV-AIDS epidemic model with memory and general incidence rate, *Eur. Phys. J. Plus.* 136(1) (2021) 1-20.
28. A. Jajarmi, B. Ghanbari and D. Baleanu, A new and efficient numerical method for the fractional modeling and optimal control of diabetes and tuberculosis co-existence, *Chaos* 29(9) (2019) 093111.
29. Y. Li, Y. Chen and I. Podlubny, Stability of fractional-order nonlinear dynamic systems: Lyapunov direct method and generalized Mittag-Leffler stability, *Comput. Math. with Appl* 59(5) (2010) 1810-1821.
30. C. Vargas-De-León, Volterra-type Lyapunov functions for fractional-order epidemic systems, *Commun. Nonlinear. Sci. Numer. Simul* 24(1-3) (2015) 75-85.
31. I. Ameen, D. Baleanu and H. M. Ali, An efficient algorithm for solving the fractional optimal control of SIRV epidemic model with a combination of vaccination and treatment, *Chaos Solitons Fractals* 137 (2020) 109892.
32. S. K. Choi, B. Kang and N. Koo, Stability for Caputo fractional differential systems, *Abstr. Appl. Anal.* 2014 (2014) 631419.
33. P. Van den Driessche and J. Watmough, Reproduction numbers and sub-threshold endemic equilibria for compartmental models of disease transmission, *Math. Biosci.* 180(1-2) (2002) 29-48.
34. J. Huo, H. Zhao and L. Zhu, The effect of vaccines on backward bifurcation in a fractional order HIV model. *Nonlinear, Anal. Real. World. Appl.* 26 (2015) 289-305.
35. L. S. Pontryagin, V. G. Boltyanskii, R. V. Gamkrelidze and E. F. Mishchenko, *The mathematical theory of optimal processes*, Gordon and Breach Science Publishers (1986).

**How to cite this article:** Ma W, Ma N, Dai C, Chen Y, and Wang X (2022), Fractional modelling and optimal control strategies for mutated COVID-19 pandemic, *Math Meth Appl Sci*, 2022;00:1–24.

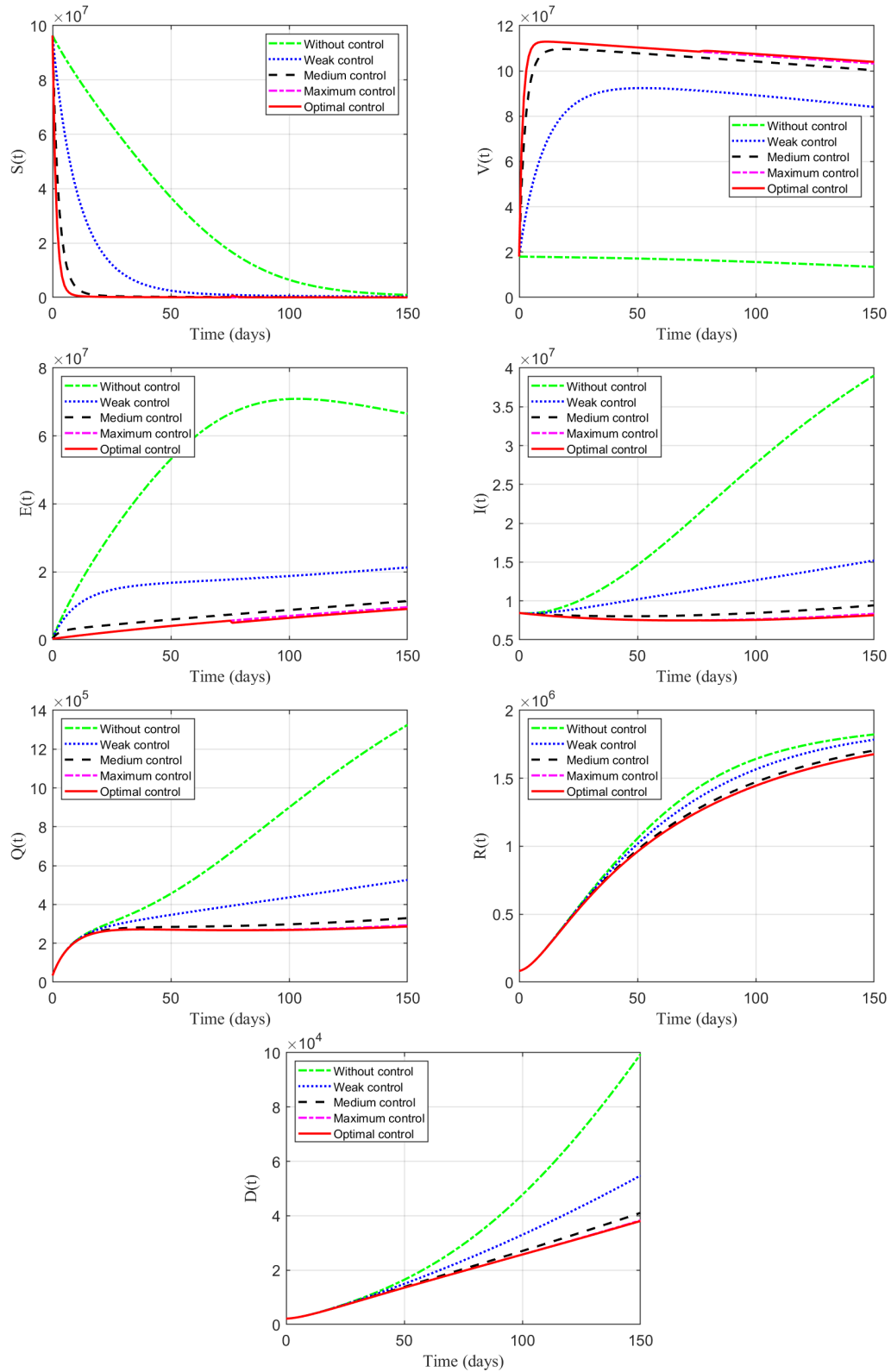


**Figure 8** When  $T=150$ , comparison between the numerical solutions of model (7) in case of without control, weak control, medium control, maximum control and optimal control

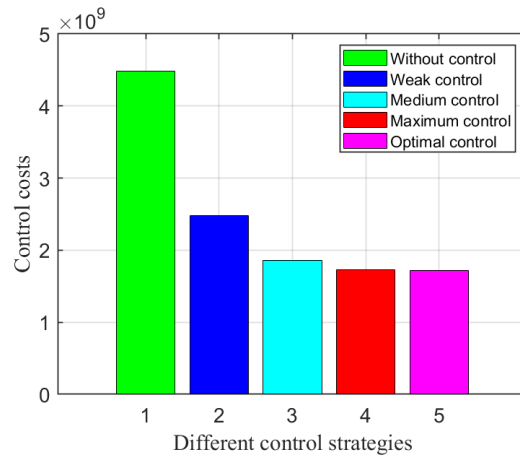


**Figure 9** Control costs of without control, weak control, medium control, optimal control and maximum control

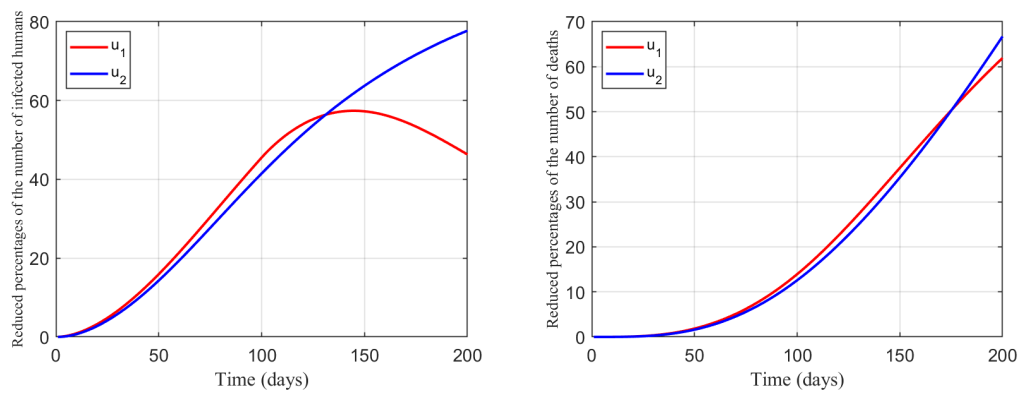


**Figure 10** Non-pharmaceutical interventions  $u_1$  and vaccination  $u_2$  reduce the percentage of the number of infected humans and deaths